Fall 12-2022

Tracer Techniques Used to Analyze Spatial and Temporal Processes Controlling Groundwater and Near Surface Water Contribution to the Ruby River in the Upper Ruby River Valley, MT.

Max-Henry Nelson

Tracer Techniques Used to Analyze Spatial and Temporal Processes Controlling Groundwater and Near Surface Water Contribution to the Ruby River in the Upper Ruby River Valley, MT.

by

Max-Henry Nelson

A thesis submitted in partial fulfillment of the
requirements for the degree of

Master's of Science in Geological Science: Hydrogeology

Montana Tech

2022

Abstract

Stable water isotopes, δD and δ18O as well as specific conductance (SC) are often used as chemical tracers, or water fluxes, to understand basin hydrological processes including precipitation, groundwater recharge, groundwater-surface water interactions. In understanding the behavior of isotopes in a natural system, quantitative models can be produced to identify volumes and sources of groundwater recharge or losses as well as how groundwater pumping and surface water irrigation affects groundwater storage and discharge. The overarching questions are: i) what are the current spatial and temporal processes controlling groundwater and surface water, ii) what are the major sources of water and iii) what is the interaction between restoration and the hydrology of the upper Ruby Valley. This study found that the upper Ruby Valley is a seasonally dynamic hydrologic system dominated by snowmelt runoff and groundwater depending on the time of year. The source-sink dynamics show significant spatial variations with many gaining and losing reaches and has a complex surface water dynamic because of numerous ditches and tributaries contributing and withdrawing from the river. While some tributaries are groundwater dominated, others are near surface water dominated. This study also suggests that there are two sources of groundwater and a near surface water contributing to the upper Ruby Valley from the three-component mixing analysis. This study suggests source of the F1-1st groundwater is most likely groundwater from irrigation return flow from ditches. The source of F2 is likely near surface water while F3-2nd groundwater is generally the upper Ruby valley groundwater. As F1-1st groundwater component is most likely from irrigation return, it can be suggested that the plug and pond restoration system will store the F2-near surface water in surface water delineations of side channels and oxbow lakes for late season signatures of the F1-1st groundwater

Keywords: Stable water isotopes, two-component mixing model, three-component mixing model

Dedication

I dedicate this to my wife, Nadia for packing up your life and taking the journey with me for this dream. Thank you for the love and support through it all.

Acknowledgements

I would like to express my most sincere gratitude to my thesis advisor and chair of my committee Dr. Glenn Shaw for the continuous feedback, vast knowledge and support from the beginning to the end. I also want to thank my thesis committee members, Dr. Robert Pal and Ronald Breitmeyer for taking this on and providing challenging ideas and invaluable expertise. Stable water isotope Analysis conducted by Jackie Timmer at the Montana Bureau of Mines and Geology

This project would not be what it is without support from Erin McGowan, Nathan Korb and The Nature Conservancy for providing the project, helping with data collection and financing this research.

Table of Contents

List of Figures

List of Equations

1. Introduction

Destruction of natural landscapes and modification of natural water regimes have led to habitat degradation or loss which contribute to 85% of the species classified as at risk in the USA (Wilcove et al.,1998; Tockner and Stanford, 2002.) Agricultural and urban development have led to pollution and drainage of water resources in 50% of the wetlands worldwide (Russi et al., 2013.) The natural water regime or river geomorphological features are the two main types of engineering controls on ecological restoration of rivers (Pan et al., 2016). Major water regimes drive many biologic nutrient cycling supporting wetland function, which in turn influences water quality and flow dynamics (Wegener et al., 2017 and Russi et al., 2013.) These ecosystem services are dependent on hydrological links such as bank overflow and groundwater flow (Kondolf et al.,2006.)

Channel incision or decreased lateral channel migration rates caused by land use changes, riparian degradation or loss of beavers can cause sedimentation and reduced surface and groundwater storage (Marston, 1994, Bufe et al., 2019.) An increase of groundwater recharge through the peak discharge season will enhance groundwater discharge into the stream during late/ low flow season. When a river has been impacted and requires restoration, a baseline analysis of the interaction between the surface and groundwater must be performed to plan how hydrologic restoration should be targeted. An incising river channel could suggest a simultaneous drop in water table which would further reduce the water available for riparian plants, reducing total biomass and river cover in turn reducing habitat (Nauburg, 2005.)

Effective long-term management of surface water for ecological restoration requires a fundamental understanding of groundwater surface water interactions (Muangthong and Shrestha, 2015. Levy and Xu, 2011). Major water regimes are influenced by both physical and

ecological factors (Russi et al., 2013). The Ecosystems of the Western United States arid and semi-arid climates supported by mountain precipitation and regional groundwater storage and flow paths. Establishing a baseline of local and regional flow paths using water fluxes is vital in understanding the natural water regime which is critical for ecological restoration (Russi et al., 2013, Shaw et al., 2014.)

Basin hydrological processes, such as precipitation, groundwater recharge, and groundwater-surface water interactions, frequently utilized as chemical tracers are stable water isotopes D and 18O as well as specific conductance (SC) (Yeh, et al. 2014). However, groundwater isotopes remain poorly understood, mostly due to the complexity of natural systems (Jasechko, 2019). Quantitative models can be created in order to identify the volumes and sources of groundwater recharge or losses, in addition to the way groundwater pumping and surface water irrigation effect groundwater storage and discharge.

1.1. Local

The focus of this study is the upper Ruby River in the South-Western portion of Montana, where restoration efforts have occurred on the lower sections and now planning for restoration of the middle section is currently under development (Figure 1). The Ruby River has been negatively impacted both hydrologically and ecologically, over the last two centuries (Boyd, 2018). The major historical impairments to the stream include beaver trapping, land development and riparian degradation. This culminated in one major flooding event in 1984 that reduced the total length of the upper Ruby by over 1.6 km (Boyd, 2018).

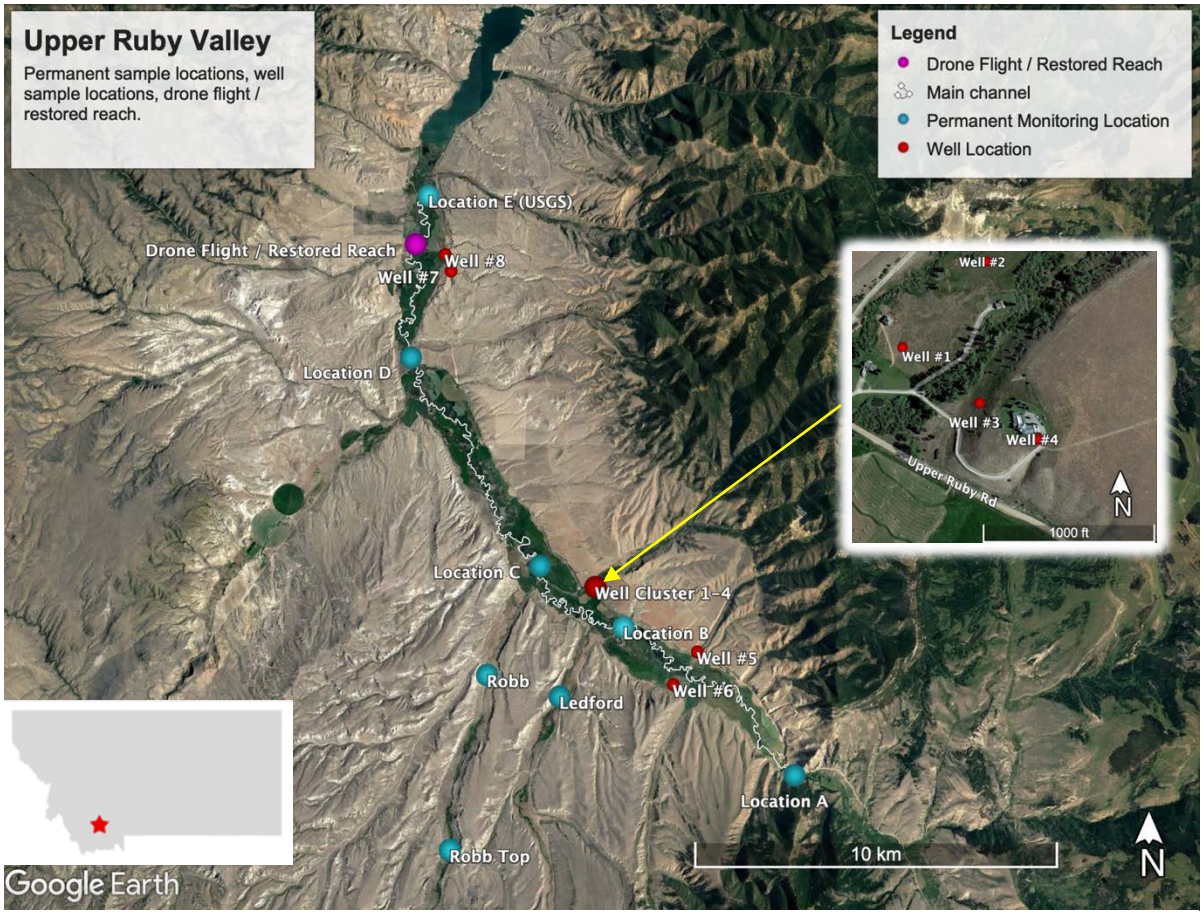

Figure 1: The Upper Ruby River valley, permanent monitoring locations, sampled well locations and drone flight / restored reach

In the upper Ruby River beaver populations were severely impacted in the early part of the 1800's. The fluvial incision and transformation from wetland complexes to a faster deeper channel are most likely due to the loss of beavers (Boyd, 2018). Land development and riparian degradation have drastically altered the channel morphology. In 1961 there were intentional cutoffs that streamlined the river. Streamlining the river increases the rivers velocity and decreases the water that can recharge the groundwater. An increased stream velocity often leads to channel incision. This is evident on the upper Ruby River, with perched extinct channels (Boyd, 2018). Most recent losses in woody riparian cover are most likely from a combination of

the channel incision and active clearing for cattle grazing. Currently, livestock access to riparian areas on a majority of the upper Ruby River is not restricted and has led to the over competition of the beaver food supply (Marston 1994).

From a geomorphological perspective, the Ruby River channel would most likely return to a healthy state naturally (Boyd 2018). However, this could take decades if not longer and would require significant erosion and sediment transport downstream. Humanmade dams and reservoirs prevent sediment transport and the Ruby Reservoir would trap a major portion of the sediment (Snyder, 2004). Structures such as rip rap have had damaging effects on the stream ecology preventing nutrient and material exchange from the water to riparian vegetation (Pan et al., 2016) Thus, restoration is necessary to prevent sediment from filling the reservoir on a shorter time scale. This study will not directly look at sediment transport, however could be used as a proxy for sediment load capabilities by looking at the flowrates of the main channel and the tributaries.

Plug and pond system is a restoration technique designed to slow river velocities such that the water table rises and causes greater infiltration of surface water into the groundwater. The restoration technique, brush bundles are live willow cuttings that are strategically placed to restabilize the riverbank with a root system as well as provide shade to the river.

In August of 2021 Plug and Pond system with brush bundles used as bank armoring was implemented on a section of the Ruby River. For this restoration effort, the main channel was rerouted into a preexisting channels and using gravel bars in the main channel to reduce the stream velocity. It was determined that gravels would be large enough to have a long-lasting effect. To prevent further channel incision, gravels were put in the cutbanks with brush bundles

laid on top and buried with surrounding soils. What is not well understood or measured is the extent that the restoration completed would most likely benefit the hydrology

1.2. Objectives

Understanding the temporal and spatial processes controlling the water regime is key in managing water in a sustainable way. Tracer analysis and surface water balances in conjunction have proven reliable methods in assessing groundwater recharge (Koeniger et al. 2016) By collecting water isotopes ($\delta^{18}O$ & δD), (SC), temperature, and flowrate data such that surface water and load balances along with two and three component mixing models can be established to assess groundwater/surface water interactions and possible sources of water. Additionally, this project will set a baseline for understanding groundwater surface water interactions and hyporheic exchange on a watershed scale and tributary flow contributions.

Addressing the natural water regime or river geomorphological features are the two main types of engineering controls on ecological restoration of rivers. (Pan et al., 2016) This project will focus on understanding the current regional hydraulic regime specifically surface and groundwater interactions. The goals of the Ruby River restoration effort are to enhance river flows in late summer, re-connect the river with the floodplain, reduce channel incision and increase the vegetation and plant cover in the riparian zone. The current restoration methods planned or being undertaken are plug and pond with bank armoring and instream gravel bars. One objective of this research is to assess the efficacy of the restoration by surface water delineations and possibly propose areas of concern or methods that may benefit the restoration goals from TNC. This project suggests that restoration will increase the water table seasonally and behave with a source/sink relationship and the goals of the restoration effort will be met because of groundwater. Finally, this project will assess the change in surface water over time

pre- and post-restoration made by The Nature Conservancy (TNC) on the Ruby River to determine the value of the restoration techniques.

Ecological restoration by engineering controls would most likely raise the water table, this could give riparian plants access to more water, promoting growth (Nauburg, 2005). This project will assess water balances, and tracers for groundwater contributions by percent and volume seasonally to understand efficacy of the valley dynamic to promote a heathy source/sink relationship and late season flowrates. This project will also collect stream temperatures along the Ruby River which will also contributes to stream health. Groundwater is generally cooler than stream temperatures suggesting more groundwater recharge would promote a healthier stream (Constantz, 2008). The overarching questions are: i) what are the current spatial and temporal processes controlling groundwater and surface water, ii) what are the major sources of water and iii) what is the interaction between restoration and the hydrology of the upper Ruby Valley

1.3. Site Description

The Ruby River is located in the Southwestern portion of Montana. The headwaters begin in the Beaverhead National Forest stretching for 122.3 km and eventually flows into the Beaverhead River. The range of this study extends for 43.5 river km and has a difference in elevation of 155m from the geologic pinch point at Location A to the USGS gauging station at Location E, above the Ruby Reservoir (Figure 1). Though the focus of the study does not extend to the headwaters, the total drainage area of 1384.1 km^2 contributes to the flows for the study (Figure 2.) The upper Ruby valley is surrounded by the Snowcrest range to the south southwest, Gravelly range to the southeast, the Greenhorn range to the northeast and the Ruby range to the northwest (Figure 2.) While the average elevation for the basin is 2,203 m, the maximum

elevation is 3216.25 m. Surrounded by mountain ranges the upper Ruby Valley is protect from harsh weather, forming a semi-arid climate with a mean annual precipitation of 54.92 cm and an average annual temperature of 2.67°C.

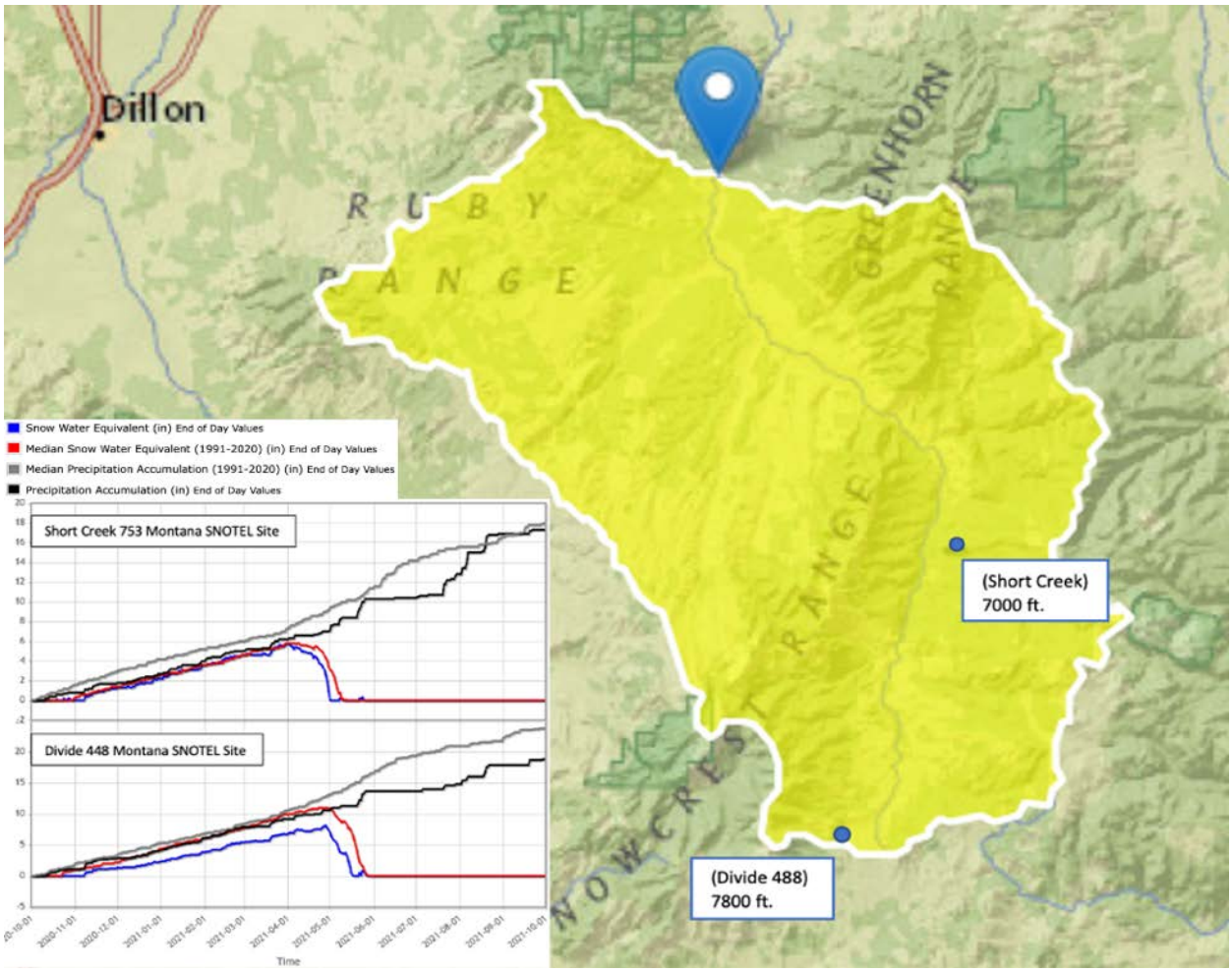

Figure 2: Drainage basin with the locations and data for 2020-2021 at the two SNOTEL sites within the basin (USDA SNOTEL and USGS stream stats)

From 1939 until 2021 the average annual flow rate at the USGS gauging station was 5.05 $m^3/_S$ (Figure 1. and USGS). There are two SNOTEL sites within the basin, both are located above the study area and do not fully encompass the seasonal snow water equivalent (SWE) for the study (Figure 2). Within the basin 24.8% of the land covered in forest however a majority of

the this is at higher elevations with mostly grassland within the valley. The lowlands within the basin are used mostly for farming cattle and bison. Irrigation ditches divert much of the water from the Ruby River to aid in field growth for said cattle and bison farming. There is also crop farming along the Ruby and the tributaries that primarily rely on groundwater wells for irrigation. Around the Ruby Rivers and tributary riparian zones is where a majority of the low land woody vegetation is prominent.

The majority of the study locations are within Quaternary alluvium, while some locations are either in or bordered by Middle Tertiary sediments or sedimentary rocks. (Figure 3.) Location A is located in Conover Ranch, Lombard, or Kibbey formation (Figure 3). The significance of the geology for this study is in the type and abundance of anions present in the groundwater produced by variable bedrock and or sediments. This in turn will affect the tracers and will need to be taken into account when doing a component mixing analysis.

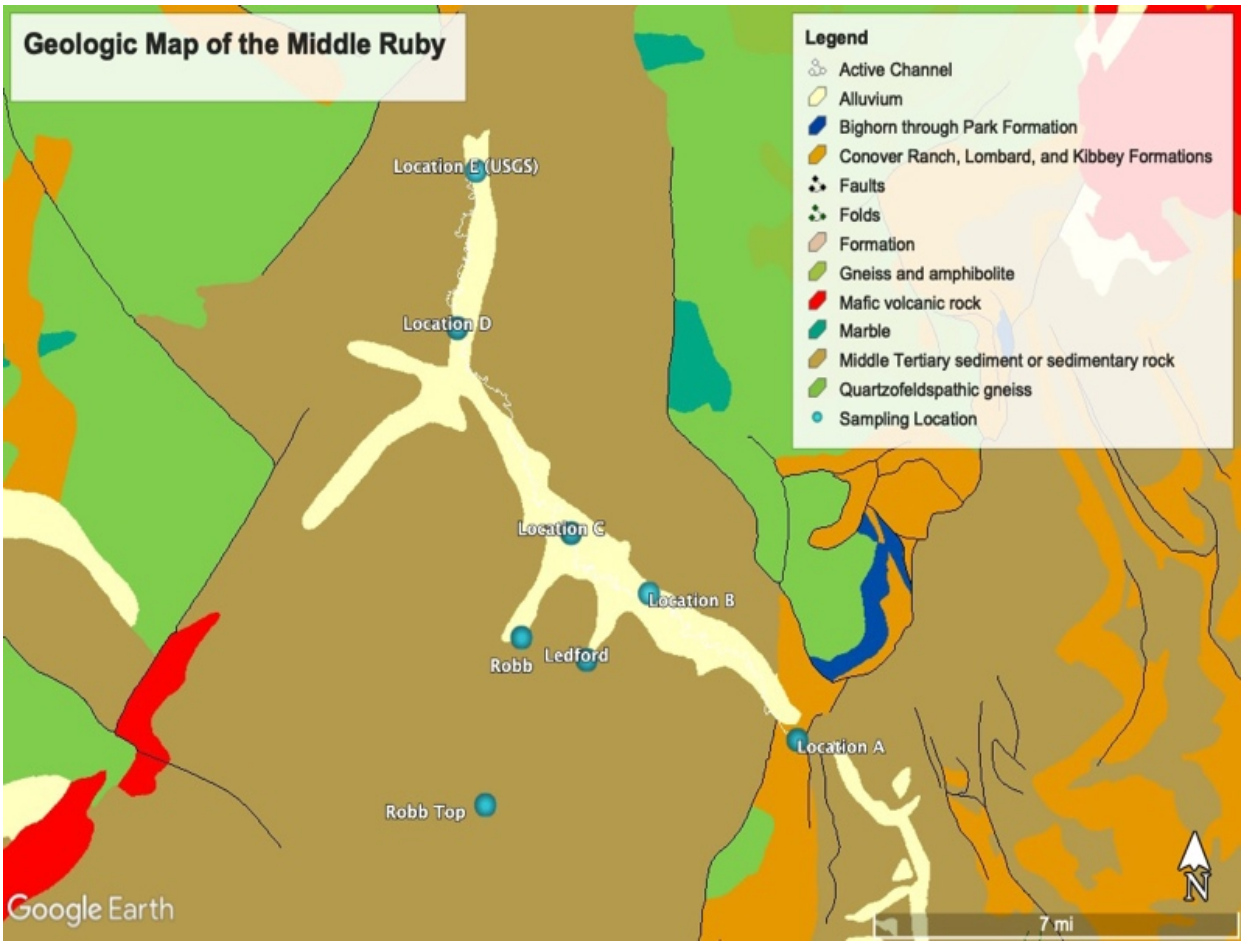

Figure 3: Geologic map (USGS) with sampling locations and Ruby River channel

2. Methods

2.1. Instruments

Stilling wells with in-situ pressure transducers and staff gauges were installed in the stream at permanent monitoring locations Ledford, Robb, Robb top, A-D, on May 27th, June 2nd, June 3rd, and June 24th respectively (Figure 1 and 4.) Pressure transducers were set to record every 15 minuets. Flowrates in the main channel were too strong to measure or install the stilling wells until the later date. In Situ Level Troll were installed, however locations C and D did not record data. Barometric pressure was recorded at each location during installation of gauging stations and recorded permanently at the Ledford location. It was assumed that the barometric pressure fluctuations would be proportional between the sites. Location E was downloaded from the USGS from June 24th and all transducer data was terminated and collected November 4th.

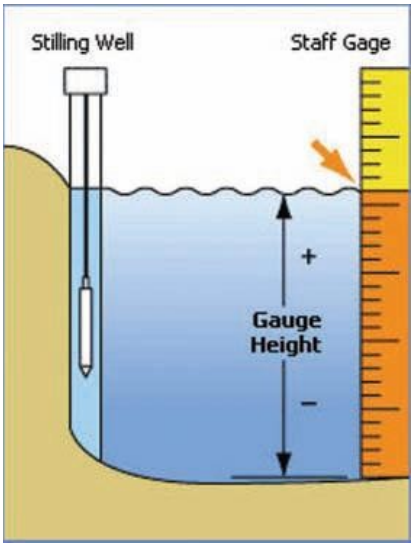

Figure 4: Representation of stilling wells with pressure transducers installed at the permanent monitoring locations

2.2. Field Methods

Manual recordings began on: May 26th at Ledford, May 27th at Robb and June 3rd at Robb top and June 25th at locations A-D. At each permanent monitoring location, the staff gauge height, river flow rate, specific conductivity (SC), temperature and a water sample were collected periodically alternating between the major tributaries (Robb, Robb Top, Ledford) and the main channel (Location A-E). At location E the staff gauge height and flow rate were not recorded because of the USGS gauging station. To measure river flow rates a transect perpendicular to the stream was constructed with a measuring tape. Flows were then taken using the Hach flowmeter at increments of 5% of the total distance. Stream profiles were saved in the Hach flowmeter and flowrates were recorded. Measurements of temperature, and SC were recorded using YSI Pro 1030. Water samples were collected without headspace in 30ml HDPE or 8ml borosilicate glass vials and were given to Montana Bureau of Mines and Geology's analytical chemistry lab to determine amount, per mil, of stable water isotopes (δ D) and δ18O relative to the VSMOW standard.

On August 31st of 2021 The Nature Conservancy (TNC) organized a synoptic flow event with 17 individuals to capture the spatial distribution of surface water. This was done mostly to analyze the complexities of the surface water in the Upper Ruby valley, as there are several ditches and small tributaries entering between long term monitoring locations. At each of the 29 surface flows that were recorded, a water sample was collected. The sample was then sent with the other collected water samples to the MBMG.

On April 24th of 2022 two drone missions, and 3 flights were conducted with a RTK Phantom 4 collecting a cross grid of aerial imagery from the 2021 restored area (Figure1).

On May 5th of 2022 eight deep groundwater wells along the upper Ruby River were sampled, tested for SC and poured into glass vials (Figure 1). Well water samples were then sent

to MBMG for analysis of stable water isotopes δD and δ^{18}O per mil ($^{0}/_{00}$), relative to the Vienna standard meteoric ocean water (VSMOW).

2.3. Data Processing

With manual flows taken and continuous stream stage, rating curves for each site were created for of the relationship between stream stage and flow rate. With the pressure transducer data collected and the rating curve, flows were calculated for every 15 minutes at each of the permanent monitoring locations. Since data was not recorded by the transducer at location D and C, a relationship between measured flowrates at locations A, B and E to locations C and D was calculated. This relationship was then used to approximate flowrates every 15 minuets relative to the flowrates calculated by transducer data and the rating curve.

A surface water balance was created for each reach between monitoring sites on the main channel. This surface water balance was represented by:

$$Q_{us} + Q_t + \Delta Q = Q_{ds} \tag{1}$$

where Q_{us} is the flowrate at the upstream location in, Q_t is the flowrate from measured tributaries in, ΔQ is the summation of inflows and outflows for groundwater and unmeasured surface water, and Q_{ds} is the flowrate at the downstream location.

Flowrates were measured in CFS and converted into $\frac{m^3}{s}$. To differentiate the source of the change in flowrate, the measured concentrations are then multiplied by the flowrate to calculate load:

$$QC = \mu \tag{2}$$

where Q is flowrate in $\frac{m^3}{s}$, C is the concentration and is usually measured in $\frac{g}{m^3}$, to calculate load (μ) in mass per time $\frac{g}{s}$. SC was measured in $\frac{\mu S}{cm}$ and without knowledge of the specific salts in the stream a ratio between TDS in $\frac{g}{m^3}$ to SC $\frac{\mu S}{cm}$ is expected to be between 0.5 and 0.9 (Hem, 1985, USGS). An approximation for concentration was used such that 1000 µS/cm is equal to a concentration of 550 $\frac{g}{m^3}$ based on average SC values and estimated ranges of SC from concentrations (Hem, 1982).

Though Location A is not at the very beginning of the river, this location is the start of the measurements and it will be assumed that this is the beginning in stream concentration and has a distance downstream of zero. All distance downstream measurements in the main channel will be relative to Location A. This is an additive and subtractive method that suggests the influence of groundwater by volume and concentration. A load balance was created for each reach between monitoring sites on the main channel. This load balance was be represented by:

$$\Delta\mu = \mu_{ds} - \mu_{us} - \mu_t \tag{3}$$

Where μ_{us} is the load at the upstream location, μ_t is the load from measured tributaries, μ_{ds} is the load at the downstream location, and $\Delta\mu$ is assumed to be change in groundwater.

The two-component mixing analysis describes the relationship between two different water sources using a mass balance of water and single tracer. SC was used as the tracer in a two-component mixing analysis for the source waters to the upper Ruby River. The uppermost permanent monitoring site was chosen as the endmember for the near-surface water component as this had the lowest SC value in May. This is justified by the fact that it is the closest to the river's headwaters, where groundwater is less likely to be present and when surface water makes

up the majority of the river's flow. The most downstream well had the highest SC and was uses for the groundwater component (Figure 1). The fractional mass balance was represented by:

$$f_1 + f_2 = 1 \quad (4)$$

$$f_1 = 1 - f_2 \quad (5)$$

$$A_1 f_1 + A_2 f_2 = A_s \quad (6)$$

where f is the fractional contribution to streamflow and A is SC. Subscripts 1, 2 and s represent groundwater, surface water and instream SC or fractional contribution respectively. Equation (5) was inserted into equation (6) to solve for fractional contribution from the different end members was solved by:

$$A_1(1 - f_2) + A_2 f_2 = A_s \quad (7)$$

$$f_2 = \frac{A_s - A_1}{A_2 - A_1} \quad (8)$$

This solution was then be used to calculate the fractional contribution for f_1 using equation (5). The fractional contributions were then multiplied by the flowrates in the stream to calculate flowrate contributions from groundwater

All water samples collected and analyzed by the MGMG were plotted on $\delta^{18}O$ vs. δD graph with the Global meteoric water line (GMWL) Butte meteoric water line. If the data plots mostly on the meteoric waterline for Butte, this data will be used as the standard for the Upper Ruby Valley Stable isotope data

The importance of the three-component mixing analysis is that it will determine if there is more complexity to the flow regime than described in the two-component system. Methodology for mixing analysis followed (Shaw et al. 2014.) SC and $\delta^{18}O$ were used as the two tracers in a mixing analysis in the first three- component mixing model while the source waters to the upper

Ruby River. The three-component mixing analysis is based on the mass balance for water and two tracers. This mass balance and fractional discharge of the stream was represented by:

$$f_1 + f_2 + f_3 = 1 \tag{9}$$

$$f_1A_1 + f_2A_2 + f_3A_3 = A_s \tag{10}$$

$$f_1B_1 + f_2B_2 + f_3B_3 = B_s \tag{11}$$

where f is the fractional contribution to streamflow from each source; A and B are the composition of the two tracers: subscripts 1,2,3 represent the 3 different sources while s represents stream water. Fractional contribution from the different end members was solved by:

$$f_1 = \frac{[(A_2B_3 - A_3B_2) + ((B_2 - B_3)A_s) + ((A_3 - A_2)B_s)]}{|-A_2B_1 + A_3B_1 + A_1B_2 - A_3B_2 - A_1B_3 + A_2B_3|} \tag{12}$$

$$f_2 = \frac{[(A_3B_1 - A_1B_3) + ((B_3 - B_1)A_s) + ((A_1 - A_3)B_s)]}{|-A_2B_1 + A_3B_1 + A_1B_2 - A_3B_2 - A_1B_3 + A_2B_3|} \tag{13}$$

$$f_3 = \frac{[(A_1B_2 - A_2B_1) + ((B_1 - B_2)A_s) + ((A_2 - A_1)B_s)]}{|-A_2B_1 + A_3B_1 + A_1B_2 - A_3B_2 - A_1B_3 + A_2B_3|} \tag{14}$$

The drone imagery from two drone missions, and 3 flights was processed through Pix4DMapper by Jim Jonas. The TIF file from the Pix4DMapper report was then uploaded into Google Earth Pro. Using Google Earth Pro's historical satellite imagery from the area, the surface water area was delineated for 1995, 2005, 2011, and 2014 as well as the 2022 drone imagery for surface water area and restoration techniques. There was more historical data, however the imagery from this data did not have the resolution to the scale needed. All of the delineations have the same ditch that comes into the river roughly in the same location. This ditch was not used in the surface water delineation.

3. Results

3.1. Flowrates

The temporal and spatial distribution of flowrates on the main channel indicates some interesting trends (Figure 5). June 24th was the first date that flow data could be safely recorded in the main channel. Typical stream morphology would suggest an increase in flowrates with progression downstream. Interestingly, at the beginning of the field season, location A had the highest flowrate, followed by location C, E, D, then B in decreasing order. Over the course of the season, the flowrate of the upper locations began to drop such that all the instream flowrates were roughly equal except location B which was still significantly lower.

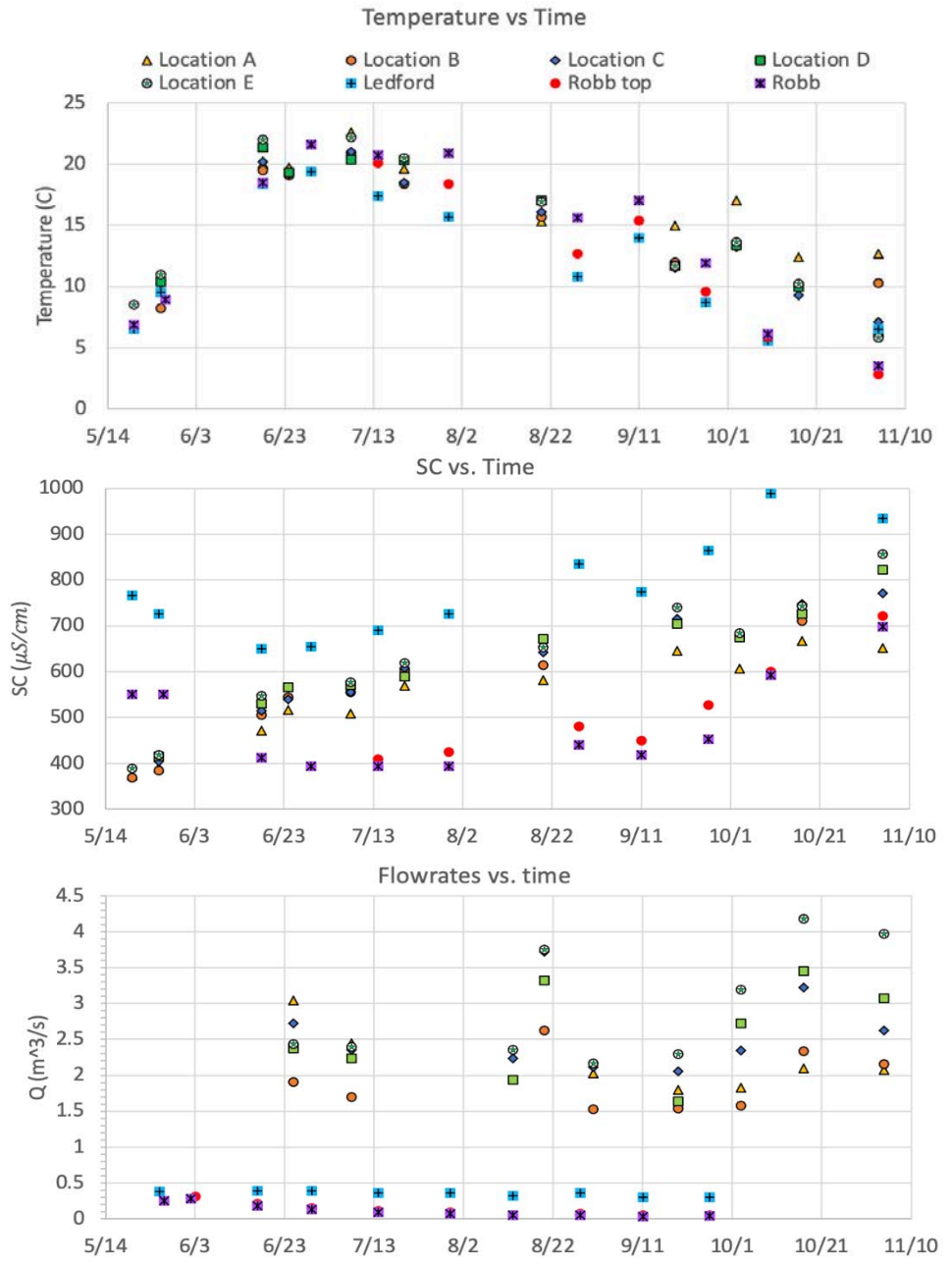

Figure 5: Field measured in stream temperature, SC, and Flowrates.

On August 8th, there were 3 distinct groups of flowrates; Locations E and C had the highest flowrates with E being slightly higher than C, Locations A and D were the next group with A being slightly higher than D, Location B was still significantly lower than the rest of the

locations. This week is an important indication, because both of the lower locations, D and E were higher than the upper locations. This is also the first week where location A no longer had the highest flowrate.

On October 3rd, the flowrates began to have more variability between the sampling sites with significantly higher flowrate at the lower locations compared to the upper locations. This is again with the exception of location B which had the lowest flowrate. At the end of the season, November 4th, the flowrates follow a typical flow regime where flowrates at locations A-E increased with distance downstream.

The tributary flowrates were sampled as early as May 26th, and have interestingly distinct distribution. After June 17th, all of the flowrates in the tributaries decrease in over the season. However, while Ledford does decrease over the season, the percentage of lost from peak flowrates on June 17th to the lowest flowrate recorded on September 26th was 22.9% (Figure 5.) Robb Creek had an upper monitoring location as well as a lower monitoring location which has a unique correlation. Typically, with progression downstream there is an increase with water volume, however this is not the trend that was observed on Robb Creek. The upper location on Robb Creek had a higher flowrate every time that both flowrates were measured on the same day. Both monitoring locations on Robb creek also had a significantly higher percentage lost than Ledford with monitoring location Robb Top loosing 81.8% and Robb loosing 85.0% from peak flowrates on June 17th to the lowest flowrate recorded on September 26th (Figure 5.)

3.2. Synoptic Flow Data

The synoptic flow data is the best spatial representation of the upper Ruby River and suggests many gaining and losing reaches along the main channel. The most upstream location used in the synoptic flow compilation along the main channel was 35 near permanent monitoring

location A, which had a flowrate of 2.030 $m^3/_s$, just above an un measured irrigation ditch (Figure 6 and 7). Approximately 1.6 km below location 35 at location 27 a flowrate of 1.024 $m^3/_s$ was removed from the main channel for Peterson ditch leaving 1.032 $m^3/_s$ in the main channel at location 28. The flowrate of Peterson ditch at location 27 combined with the main channel at location 28 was 0.026 $m^3/_s$ more than location 35. This increase in flowrate could be from groundwater contribution or unmeasured surface water.

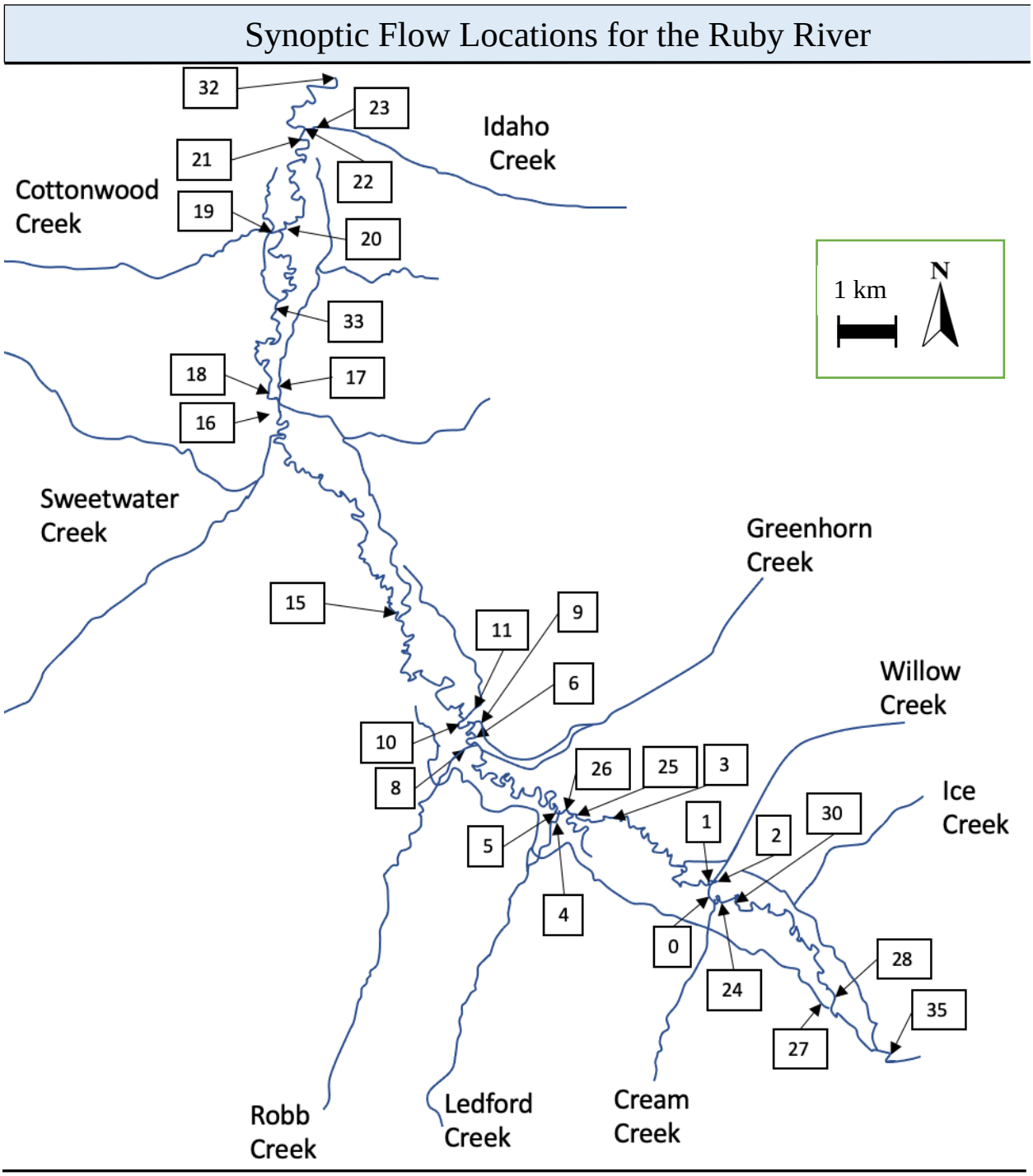

Figure 6: Synoptic flow locations.

Id	Location descriptions in the downstream direction	Discharge (m^3/s)	Change in Ruby River flows (m^3/s)	Net gains/ losses from unmeasured sources (m^3/s)
35	Ruby River above ditch near notch	2.030		
27	Peterson Ditch	-1.024		
28	Ruby River below Peterson Ditch	1.032	-0.998	0.026
30	Ruby River by Cream Creek irrigation fields downstream of Ice Creek	1.139	0.108	0.108
24	Ruby River above Cream Creek	1.087	-0.052	-0.052
0	Ruby River below Cream Creek	1.354	0.267	
2	Ruby River Above Willow Creek fork	1.293	-0.061	-0.061
1	Ruby River Below Willow Creek fork	1.499	0.206	
3	Ruby River at location B	1.526	0.027	
25	Ruby River above secondary channel	1.657	0.131	0.131
26	Ruby River secondary channel by Ledford Creek	0.208		
4	Ledford Creek	0.114		
8	Robb Creek	0.017		
6	Ruby River below Greenhorn and Robb Creek fork	1.784	0.127	0.205
9	Downstream fork of Greenhorn Creek	0.047		
10	Ruby River at location C	2.123	0.339	0.292
11	Ditch below Location C	-0.099		
15	Ruby below ditch by Donegan Slough	2.212	0.089	
16	River left ditch by Sweetwater road	-0.025		
17	Pioneer ditch by Sweetwater road	-0.556		
18	Ruby river at location D	1.813	-0.398	0.183
33	Ruby River above W. Metzel Ditch	1.781	-0.032	
19	Cottonwood Creek fork	0.000		
20	Ruby River below Cottonwood Creek fork	1.919	0.138	0.137
21	Ruby River at location E (USGS guaging station)	2.270	0.351	0.351
22	Ruby River above Idaho Creek	2.188	-0.082	-0.082
23	Idaho Creek	0.006		
32	Inflow into Ruby Reservoir	2.272	0.084	0.078

Figure 7: Synoptic flowrates from locations recorded in downstream order.

Description: Adapted from Erin McGowin at the nature conservancy. Green rows indicate main channel locations. Negative values in discharge not in the main channel indicate ditches removing water from the main channel indicate ditches removing water from the main channel. Samples/ locations 12, 13, and 14 were not sampled and a flowrate was not collected. Samples/ locations 5,7,29, and 34 were not on used for the synoptic surface water balance because the flowrate was either not taken or was unrealistic from field observations but were analyzed for isotopes

The synoptic flow location 3 was at the permanent monitoring location B and had a flowrate of 1.526 $m^3/_s$. The synoptic flow data suggests a combined contribution of 0.580 $m^3/_s$ from Willow creek, Ice creek and Cream creek. The deficit in flowrate from location 28, plus the tributary contribution, to 3 of 0.086 $m^3/_s$ could be loss to groundwater or unmeasured surface water. Just below the Location B a secondary Ruby River channel was observed contributing to the main channel, however where this secondary channel diverted from the channel was not observed. Right above this secondary Ruby River channel, the flowrate was 1.657 $m^3/_s$ at location 25 on the main channel. This is an increase from location 3 by 0.131 $m^3/_s$ that was not accounted for by observed surface water.

Location 10 in the synoptic flow was located at the permanent monitoring location C and had a flowrate of 2.123 $m^3/_s$. From location 25 to 10 the flowrate increased by 0.466 $m^3/_s$, 0.386 $m^3/_s$ of which could be accounted for with the combined flowrate from the secondary Ruby channel with Ledford creek, Robb creek and Greenhorn creek. Just below location 10, 0.099 $m^3/_s$ was removed from the main channel by a ditch. At location 15 below another ditch, the flowrate was 2.212 $m^3/_s$ for a net gain of 0.188 $m^3/_s$ from location 10, minus the flowrate of the ditch below location 10.

The ditch above location 15 comes back into the main channel right at Sweetwater bridge. Pioneer ditch at location 17 comes off the main channel on the Northeast side at 0.556 $m^3/_s$. while at location 16 on the Southwest side of the main channel another irrigation ditch directs 0.025 $m^3/_s$ from the main channel right before location 18 which was located at

permanent monitoring location D and measured $1.813\ {}^{m^3}/_{S}$. From location 15 to 18 the river had a loss of 0.398 ${}^{m^3}/_{S}$ for a net gain of 0.183 ${}^{m^3}/_{S}$ from unmeasured sources.

Just above Metzel ditch the main channel had 1.781 ${}^{m^3}/_{S}$ at location 33, a loss of $0.032\ {}^{m^3}/_{S}$ from location 18. Location 21at the permanent monitoring location E and the USGS gauging station had a flowrate of $2.270\ {}^{m^3}/_{S}$ for an increase of $0.488\ {}^{m^3}/_{S}$ into the main channel after location 33 from unmeasured sources.

Idaho creek at location 23 had a flowrate of $0.006\ {}^{m^3}/_{S}$ and though the main channel has a slightly reduced flowrate at location 22 before Idaho creek. The inlet to the reservoir at location 32 had a flowrate of $2.272\ {}^{m^3}/_{S}$, which was a net loss from location 21 of $0.004\ {}^{m^3}/_{S}$ and an overall gain from the most upstream location 35 of $0.242\ {}^{m^3}/_{S}$. Measured irrigation ditches pulled $1.654\ {}^{m^3}/_{S}$ from the main channel while measured ditches and tributaries attributed to $0.972\ {}^{m^3}/_{S}$ for the main channel flowrate. Though this does not account for all ditches and tributaries along the 43.5 km of river length. Specifically, the ditch that comes back into the river before location 18 is not measured. Additionally, the ditch that removes water from the main channel just below location 35 was not measured though field observations.

3.3. Stable Isotopes

The isotopic relationship between δD vs. $\delta 18O$ has some significant characteristics (Figure 8). The local meteoric water line LMWL (δD = 8.16 δ18O+ 8.16) for the upper Ruby River valley was established in Bailey et al. by collected monthly precipitation isotopes from 2017-2018 (Bailey et al 2022). However, the Butte meteoric water line Butte MWL (δD = 7.31δ18O − 7.5) was established in Gammons et al. 2006 and plots very similarly to the LMWL. This can be used as a reference for the upper ruby valley as this is the most well

established LMWL for the region, as well as the close proximity and similar local weather patterns. The global meteoric water line GMWL was also plotted with isotopic distributions as a comparison to global averages. Mostly the isotopic composition fell above the Butte MWL and below the GMWL. Meaning that mostly the instream samples are depleted compared to the Butte MWL and enriched compared to the GMWL. The well data is significantly more depleted in δD and $\delta 18O$ than the instream isotopic distribution. The tributaries have a general cluster for each tributary. There is a lack of grouping to a specific composition for any of the main channel locations, though these samples vary through time. The synoptic flow data does not vary through time but also doesn't group together based on where the data was taken (Figures 6 and 8).

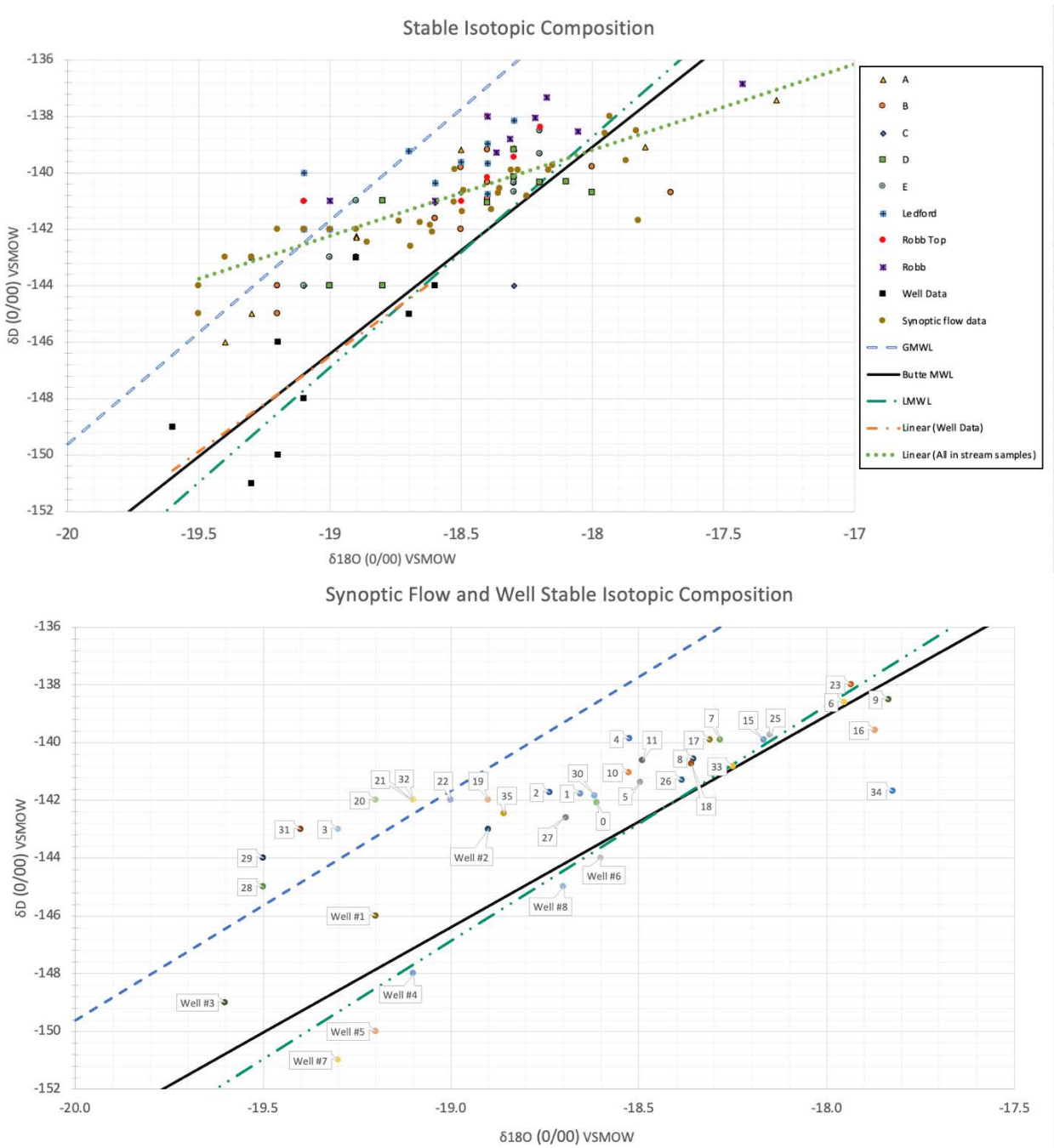

Figure 8: Isotopic distribution of δD vs. δ18O

Description: (Above): All Data. (Below): Calls out well and synoptic flow locations in relation to Figure 1 and 6. The GMWL used was: δD = 7.39 δ18O+ 8.99 (Jasechko, 2019). The Butte MWL equation used was: δD = 7.31δ18O − 7.5 established in Gammons et al. 2006. The LMWL was established in Bailey et al. 2022 was: δD = 8.16 δ18O+ 8.16.

The isotopic composition over time has very similar trends between δD vs. time and $\delta 18O$ vs. time (Figure 9). Overall, from May into November, the main channels and tributaries became more depleted in both δD and $\delta 18O$. In May the most enriched sources were Robb creek and location A. By mid-June location A was the most depleted compared to the other main channel locations, in both isotopes. While Robb remained the most depleted a majority of the time. From June until October locations D and E were usually the most enriched.

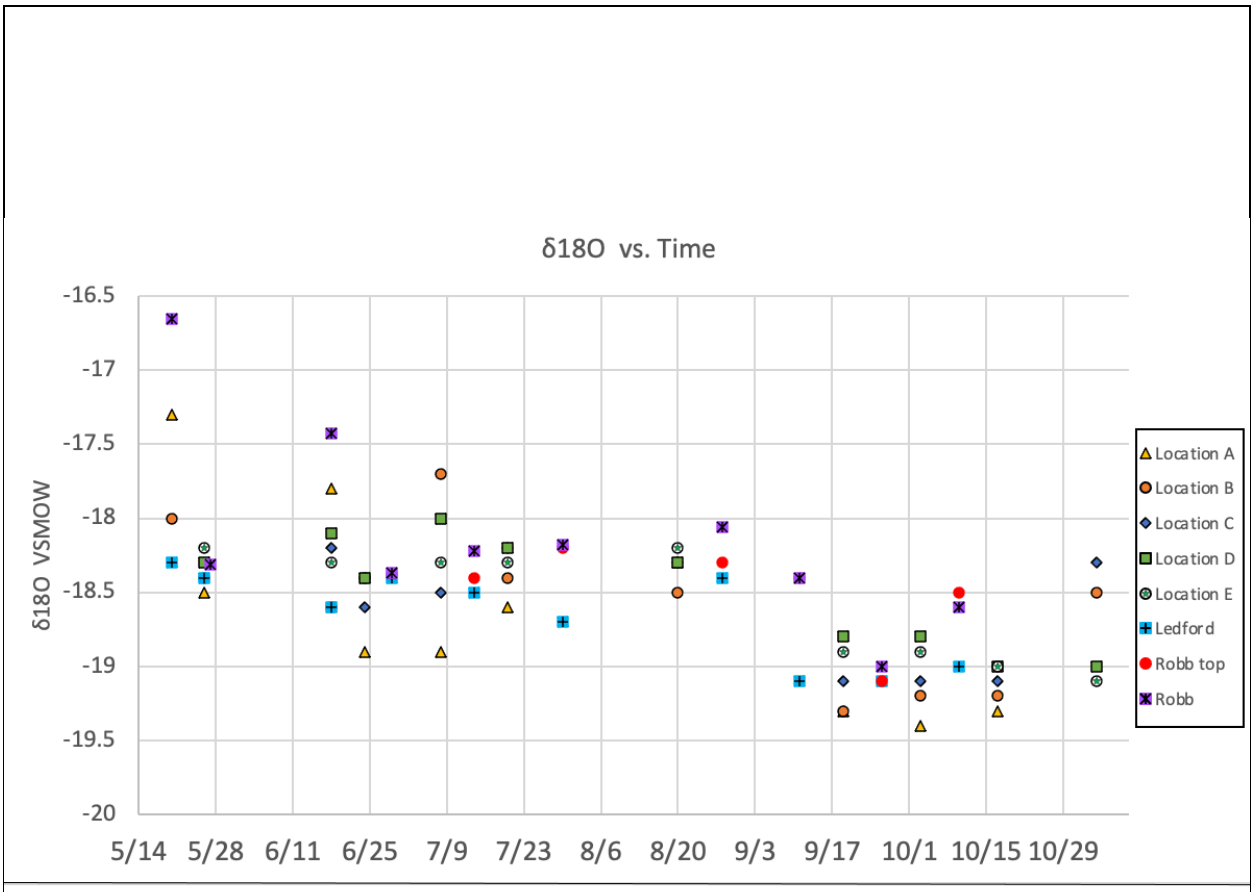

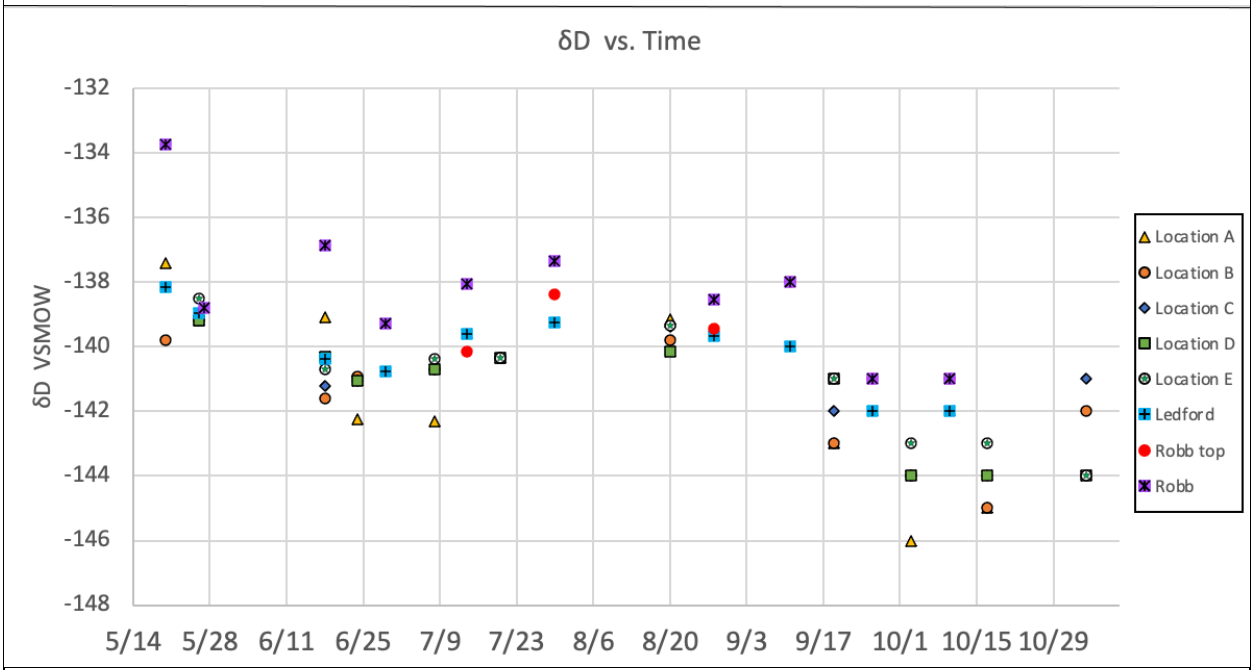

Figure 9: Change in isotopic composition of δD and δ18O over time.

3.4. Continuous Flowrate

Flowrates and stages manually taken in the field were plotted against one another to form a rating curve (Figure 10). The rating curve equation was used to calculate continuous flowrate using the 15-minute intervals of stages recorded using the pressure transducer data (Figure 12). Location E is located at the USGS Gauging station such that the continuous flowrate was downloaded and was not manually measured. However, Location C and D had pressure transducer failure and the rating curve could not be used. A correlation to a constant flowrate at a different location was necessary to calculate constant flowrate (Figure 11). The correlation compared manual flowrates at all the continuous stations to the manual flowrate of both locations C and D on the same day. The linear trendline equation was used to calculate the flowrate at locations C and D with the trendline that had the highest R^2 value. Location C best correlated linearly to location B with an R^2 value of 0.9298 while location D best correlated linearly to location E with an R^2 value of 0.8894 (Figure 11). The date and time used for locations C and D continuous flowrate was the date and time corresponding to the flowrate used from locations B and E respectively.

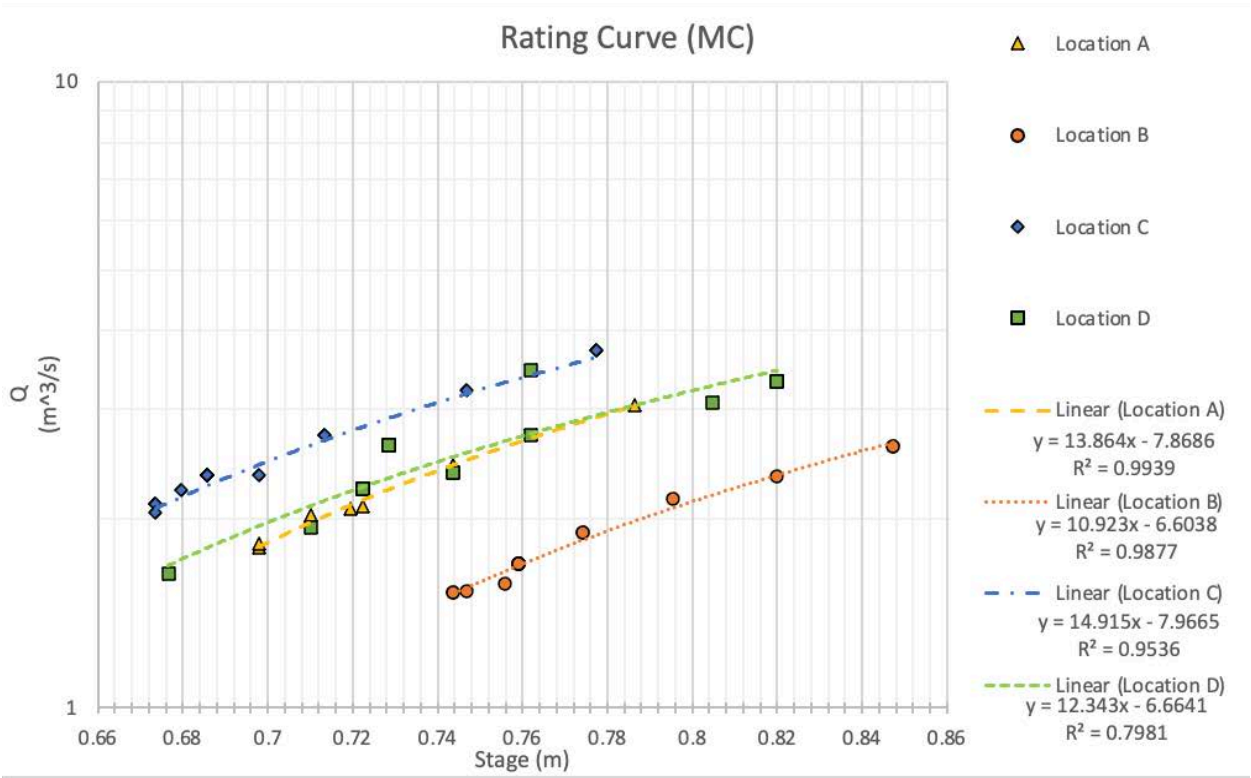

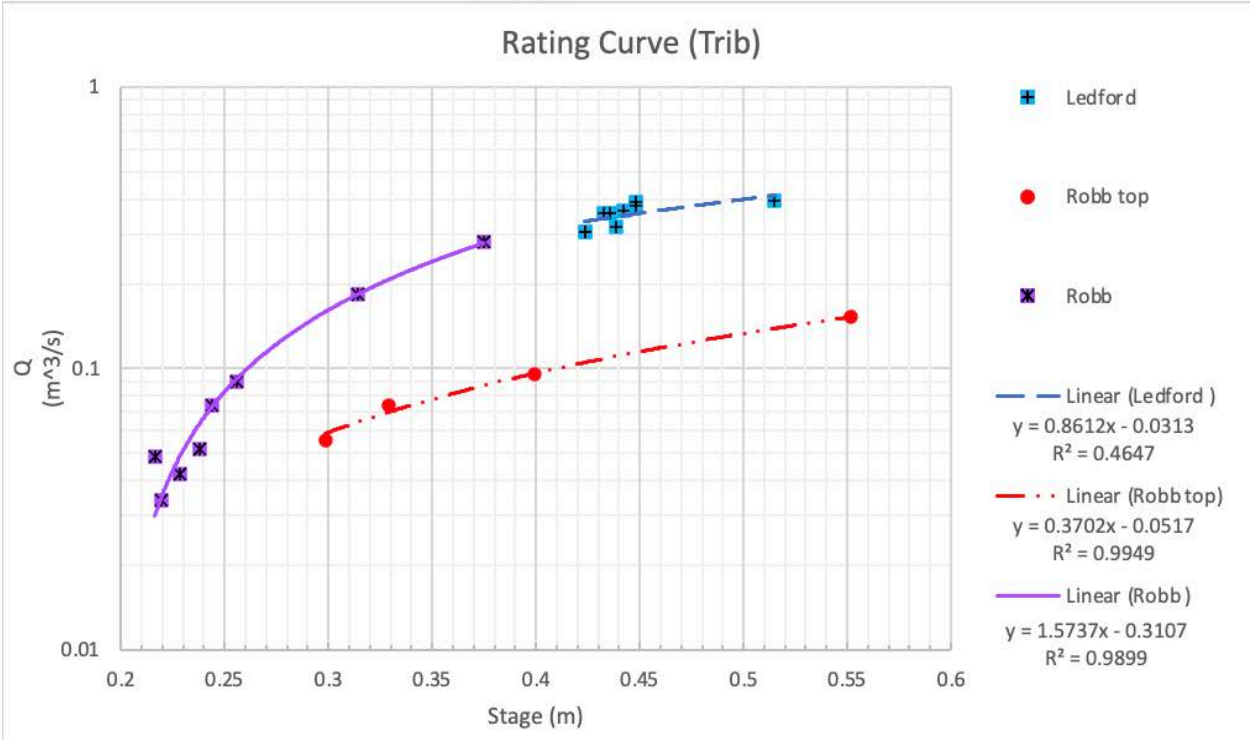

Figure 10: Rating curve, correlating stage to measured flowrates for the main channel (MC) and Tributary (Trib).

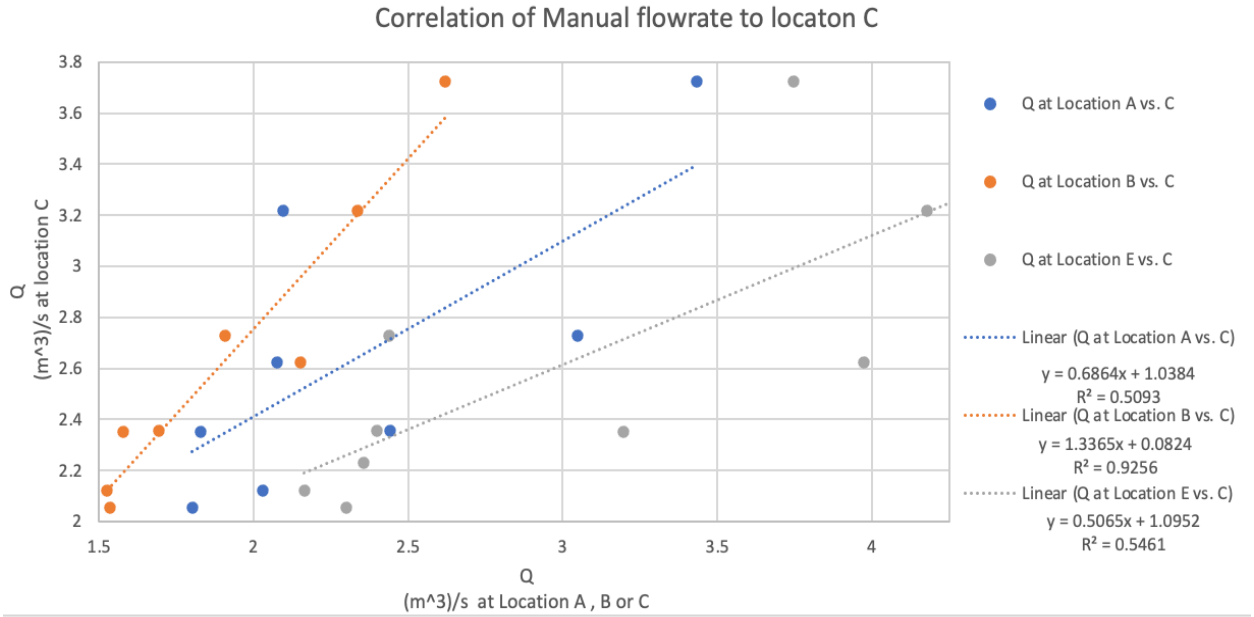

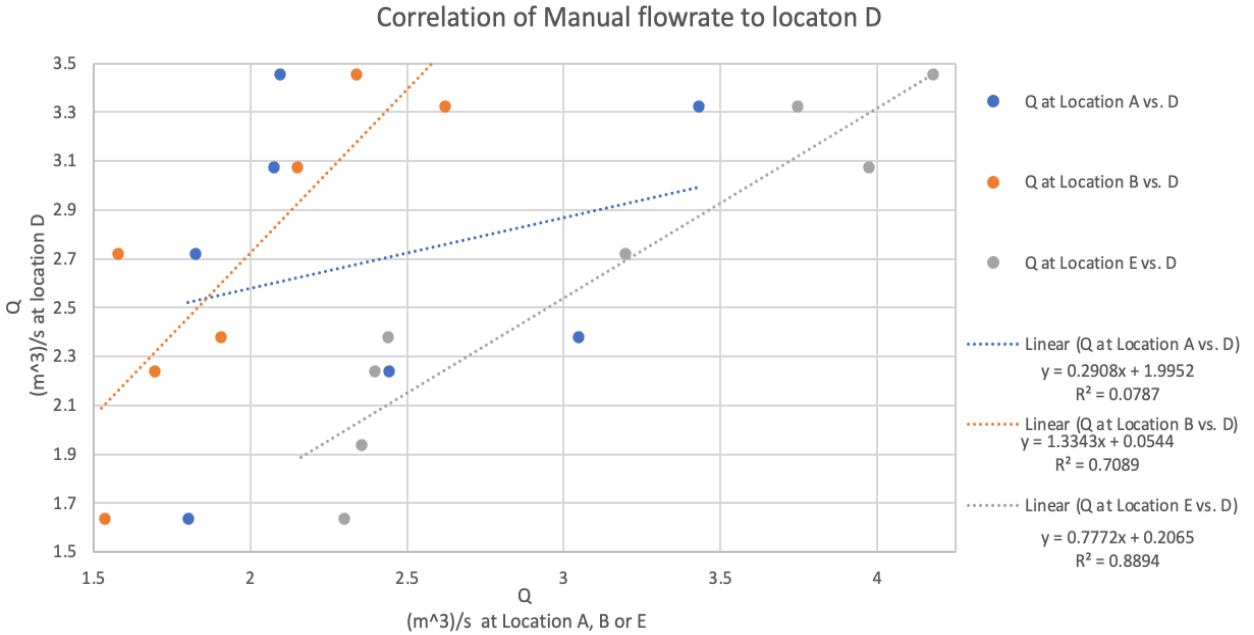

Figure 11: Correlation between manually recorded flowrates.

Description: (Above) location C (Below) location D. The linear trendline with the best fit, highest R^2 value, was used to calculate constant flowrate (Figure 12).

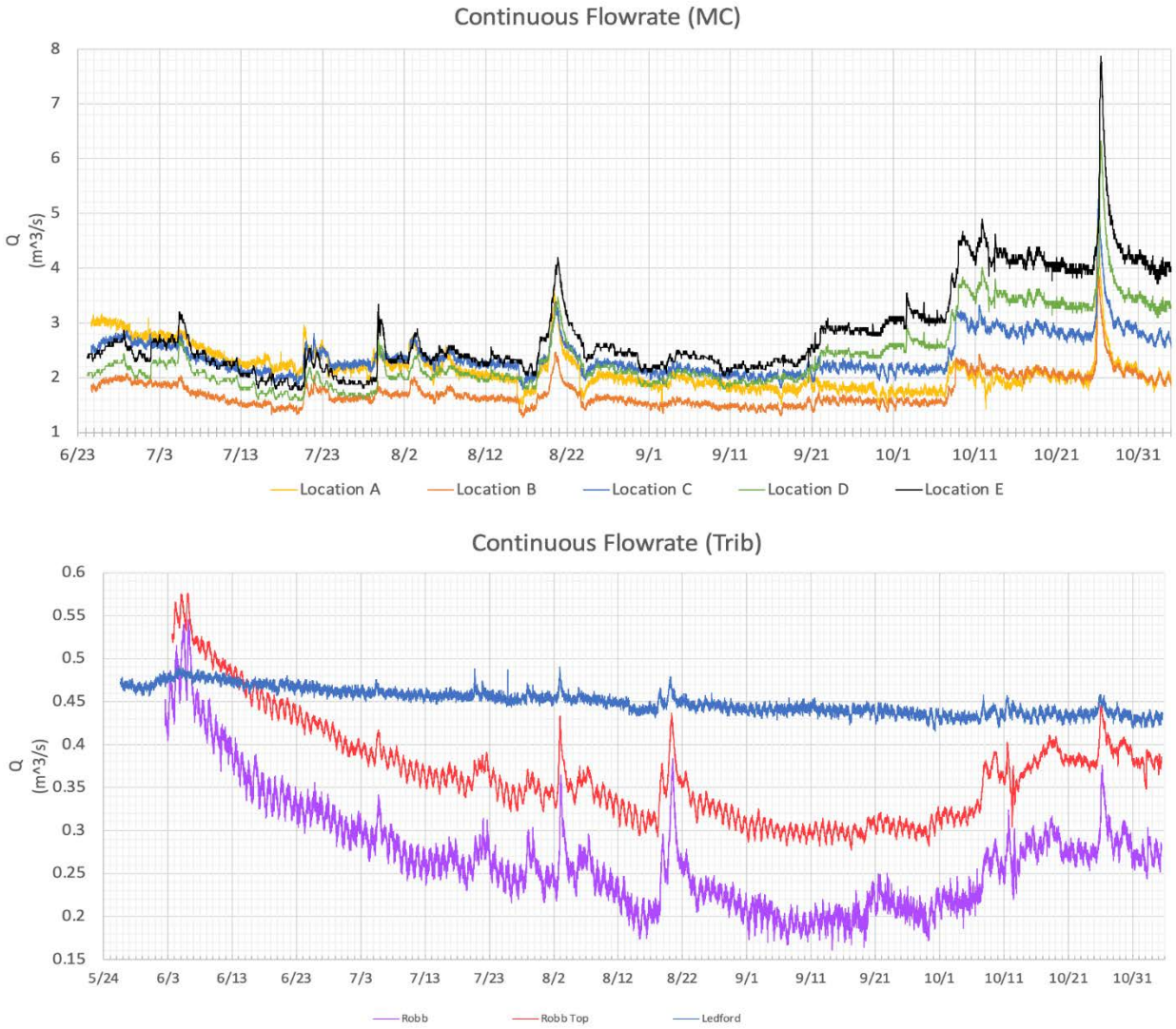

Figure 12: Continuous flowrates for all locations

Description: Locations A and B flowrates were calculated using a linear rating curve equation from manual flow and stage measurements (Figure 10) applied to stages recordings every 15 minuets from pressure transducers. Location E was downloaded from the USGS Gauging station. Location Cand D had pressure transducer failure, such that a correlation to a constant flowrate at a different location was necessary to calculate continuous flowrate (Figure 11). A linear trendline equation was used to calculate the flowrate at locations C and D with the trendline that had the highest R^2 value. Location C best correlated linearly to location B while location D best correlated linearly to location E. The date and time used for locations C and D continuous flowrate was the date and time corresponding to the flowrate used from locations B and E respectively

The trends of the constant flowrate at each location had a similar relationship between sites and throughout time to the manual flowrates. At the beginning of the season location A had the highest flowrate with a decreasing flowrate in the order of C, E, D, and then B. The constant flowrate depicts when there were storm events and the relationship between flowrates along the river where the manual flowrates does not. For small storm events before July 29th such as on July 20th-23rd the beginning of the season flow relationship is held constant where the highest flowrate is at location A with a decreasing flowrate in the order of C, E, D, and then B. However, a larger event such as the storm event from July 5th increased the lower locations flowrates more than upper locations such that the flowrate at location E was higher than the other locations. During this event, the flowrate at A, C and D were very similar.

The second distinct time period was between July 30th through September 21st. Location E had the highest flowrate with a decreasing flowrate in the order of C, D, A, and then B. However, from July 29th until August 12th location A had slightly higher flowrate than location B.

The last distinct timeline was between September 21st through the end of flowrate data collection on November 4th where the flowrate increased with distance downstream such that location E had the highest flowrate with decreasing flowrate in the order of D, C, B, and then A. However, from September 21st until October 8th location A had slightly higher flowrate than location B. This time period is distinct as there is more of a difference in flowrate at each of the locations along the river and the basal flowrate for locations C, D, and E are significantly higher than at the beginning of the season.

3.5. Surface Water Balance and Load Balance

The variability surface water balance has distinct distribution spatially and temporally over the course of the season. From June 25th through October 3rd reach A-B was a losing reach. However, the volume lost was from reach A-B progressively less until October 17th when it became a gaining reach (Figure 13.) Reach B-C was a gaining reach throughout the season. The change in flowrate within the reach peaked in late August. Reach C-D was consistently losing until October 3rd when it became a gaining reach. Reach D-E was consistently a gaining reach and generally increased in volume throughout the season.

Figure 13: Chang in flowrate and change in load per reach

Description:Calculated Load using a multiplier of 0.55 x SC as an estimate for concentration (Hem, 1985). Average tributary flowrate from previous and following week was used because flows were not recorded for the weeks main channel flows were taken. Lower Robb Creek value was used as this is more likely the volume contributed to main channel from tributary. SC from June 24th and flows from June 25th were used to calculate load on June 24th

The change in load per reach followed a similar trend as change in flowrate per reach because the load used flowrate to calculate load. However, there are some interesting distinctions from the change in flowrate and change in load. Reach A-B had the highest magnitude of change in flowrate but did not have the highest magnitude of load. Additionally, the magnitude for reach B-C was significantly higher for change in flowrate compared to the change in load throughout the season. On October 17th reach B-C had a higher gain in flowrate than both reach A-B and C-D. However, reach B-C had a lower gain in load than both reach A-B and C-D

3.6. Two-Component Mixing Model

The two-component mixing model compared the contributions of groundwater and near surface water using SC as the tracer. The uppermost permanent monitoring location, had the lowest SC value in May, and was used as the near-surface water endmember. We justify this because it is the closest to the headwaters when the majority of river flow is most likely consists of nearly all near surface water rather than groundwater. The groundwater component was set as the highest SC and was the furthest downstream location from the well data collection, located at well 8 (Figure 1)

The beginning of the data collection had between 85-100% of near surface water at all locations along main channel and between 0-15% of groundwater (Figure 14). The percentage of near surface water decreases while the percentage of groundwater had an inverse relationship and increased from the beginning to the end of the data collection (Figure 14). This correlated directly to the flowrate contribution to the main channel from groundwater and near surface water (Figure 15). At the beginning of data collection, the main channel data was clustered together, while at the end of the data collection, there was more separation and difference between percent contributions from groundwater and near surface water. At the end of the

season, the difference in groundwater contribution seemed to be the cause as near surface water contributions by volume was roughly the same at all locations along the main channel (Figure 15). Throughout the data collection, location D or E had the highest percentage of groundwater and the lowest percentage of near surface water. While these locations had the highest percentage of groundwater and the highest flowrate of groundwater, they were about average for near surface water flowrate except in October when they also had the highest flowrate for near surface water (Figure 15). Location A had the lowest percentage of groundwater and the highest percentage of near surface water throughout the data collection except for in May, when location B had a higher near surface water percentage and a lower groundwater percentage.

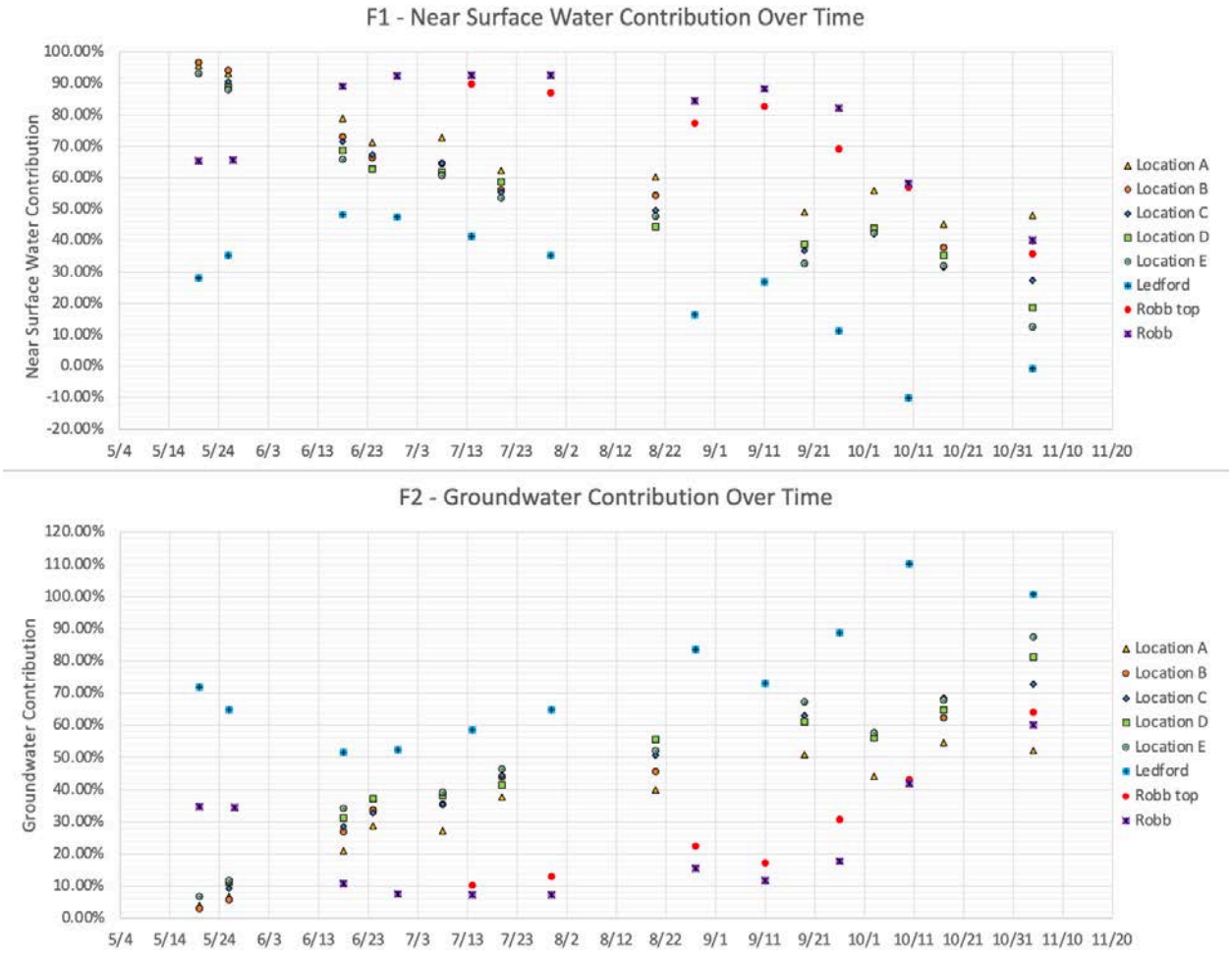

Figure 14: Percent contribution from the two-component mixing analysis

Description: Using SC as the tracer. A1 (near surface water) was calculated slightly lower than the lowest SC at 350 µS⁄cm. A2 (Groundwater) was calculated from the highest SC recorded from well data at 930 µS⁄cm

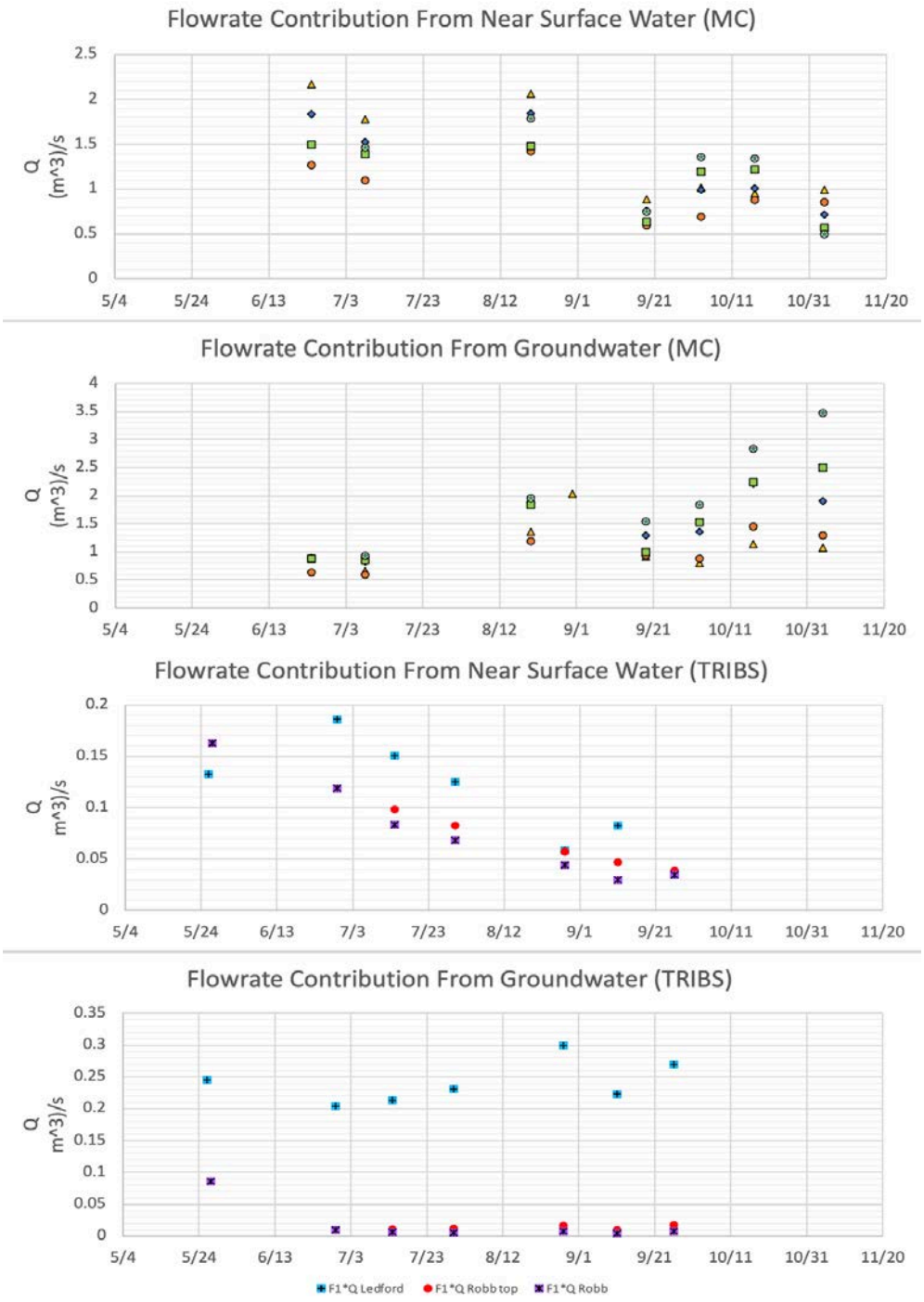

Figure 15: Flowrate from both groundwater and surface water for both the tributaries (TRIBS) and the main channel (MC)

The tributary data is distinct from the main channel data. Ledford consistently had the lowest percentage of near surface water and the highest percentage of groundwater contribution. There were two dates where the SC at Ledford was greater than the highest well SC value. This suggested that the percentage of groundwater was greater than 100% and in turn suggested that the contribution from near surface water was less than 0% (Figure 14). At all of the tributaries, the volume of near surface water decreased throughout the data collection with the exception of Ledford increasing after May. However, the flowrate of groundwater at Ledford was fairly consistent between 0.15 - 0.27 m^3/s. Rob creek was initially 0.7 m^3/s in May (Figure 15). Robb Creek had the highest percent contribution from near surface water and the lowest percent of groundwater throughout the data collection except for in May and November. The upper location of Robb creek always had more groundwater contribution and less near surface water contribution than the lower location (Figure 14). Though the upper location had slightly more groundwater flowrate, both locations remained less than 0.2m^3/s

When the two-component mixing model is applied to all of the SC values collected from the wells, the percent contribution is not majority groundwater for most of the wells (Figure 16). Wells 1, 2, 3, 5 and 7 had a majority contribution from near surface water while only wells 4, 6 and 8 had a majority groundwater contribution. Only well 8 had a groundwater contribution above 70%. The well with the highest near surface water contribution was well 7 at nearly 82%. Spatially well 7 and 8 are located closest to each other and are significantly further downstream to the other well locations (Figure 1). The high percentage of near surface water contribution within the wells may indicate more complexity to the hydrologic system.

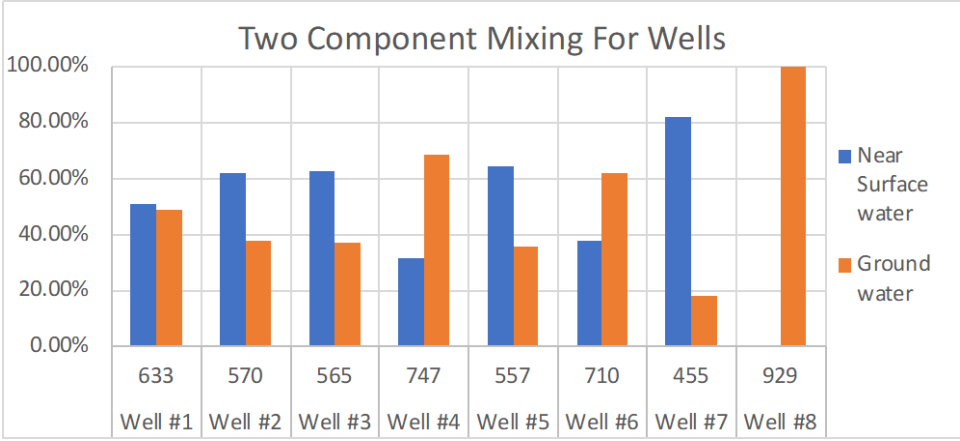

Figure 16:Percentage of near surface water and ground in the wells from the two-component mixing model.

3.7. Three-Component Mixing Models

SC was plotted against $\delta 18O$ ‰ $VSMOW$ and against δD ‰ $VSMOW$ to determine the values for the endmembers (Figure 17). For both models, a triangle was superimposed over the graph to group the data. The well data in both models' trends along the F1 to F2 line. With the SC vs. $\delta 18O$ graph, the data is more dispersed between the 3 components while in the SC vs. δD except for the well data, the data is more centralized around a trendline from F3 to some point between F1 and F2. Ledford, location D and location E cluster more towards F3, while Robb and Robb Top stay clustered between F1 and F2. All locations have a negative trendline toward different ratio of component F1 and F3. The values for the geochemical parameters for each end component derived from Figure 17 were used in equations 12-14 (Table 1).

Table I: Geochemical Parameters for Three-component Mixing Models

Model	A1	B1	A2	B2	A3	**B3**
Model 1 (SC vs. $\delta 18O$)	440.0	-19.8	325.0	-17.1	1060.0	18.9
Model 2 (SC vs. δD)	440.0	-19.8	325.0	-17.1	1060.0	18.9

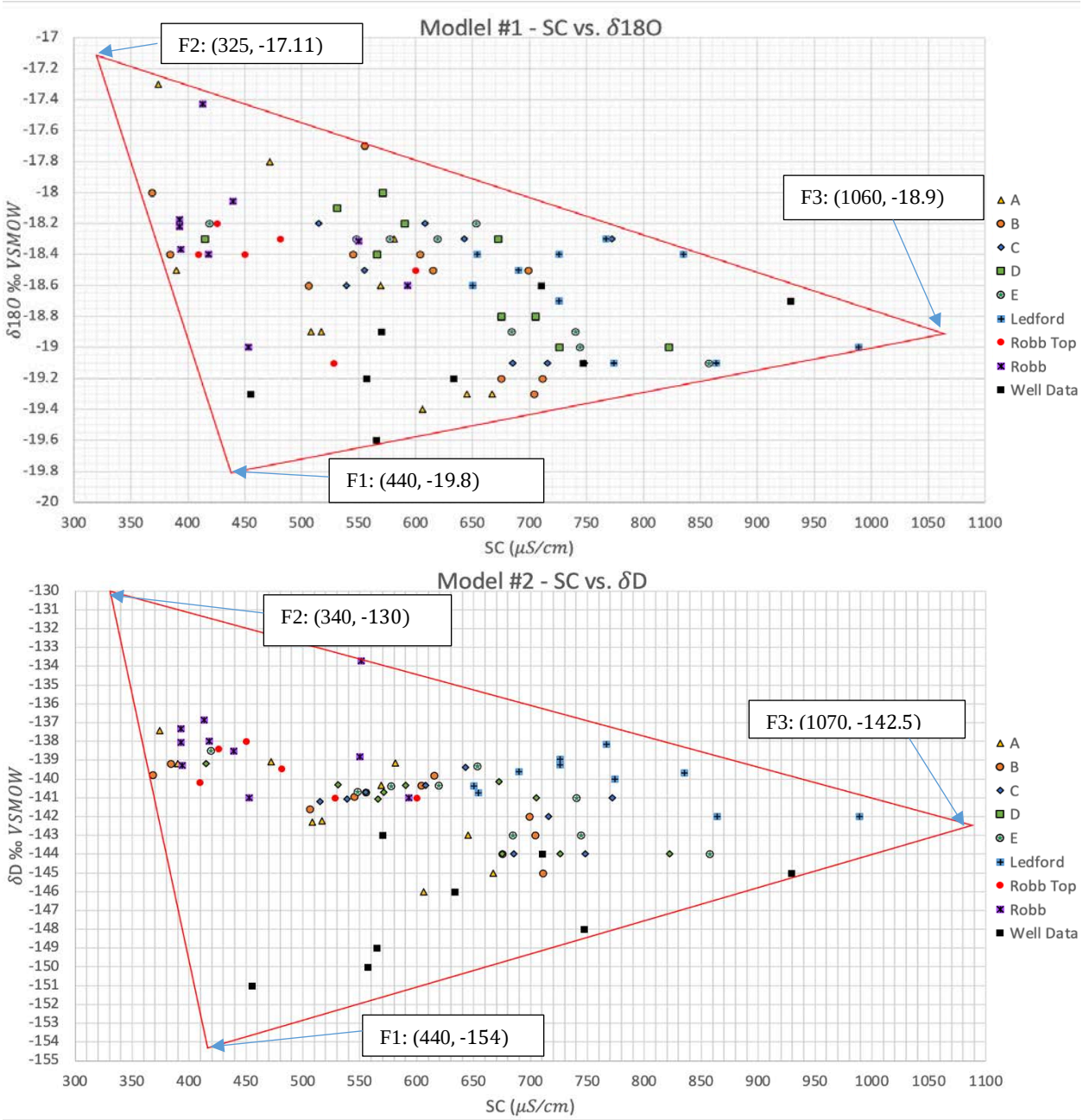

Figure 17: Model #1-SC plotted against δ18O ‰ VSMOW and Model #2-SC plotted against δD ‰ VSMOW.

Description: A triangle was superimposed over Both models to determine the values for the components of the models.

The assumption was made that the well data would be predominantly ground water. In both models, the well data generally plots along the F1 to F3 mixing line suggesting that there are two sources of ground water (Figure 17 and 18). Though the percent contribution is not the exact same between the models for the different sources, the wells typically have the same general composition between the models. In both models, wells 1, 2, 3, 5 and 7 are mostly the 1st groundwater and have similar percentages between the two models for this source. In both models well 6 and well 8 have a majority composition of 2nd groundwater. In model #1, well 4 has a majority contribution from the 2nd groundwater while in model #2 the percentage contribution from the 2nd groundwater is the same as in model #1, the slight majority is the 1st groundwater. There is some variation between the models for near surface water contributions into the well. Generally, model #2 has less near surface water contribution for all of the wells. However, wells 1 and 2 both have higher near surface water contribution than in model #1.

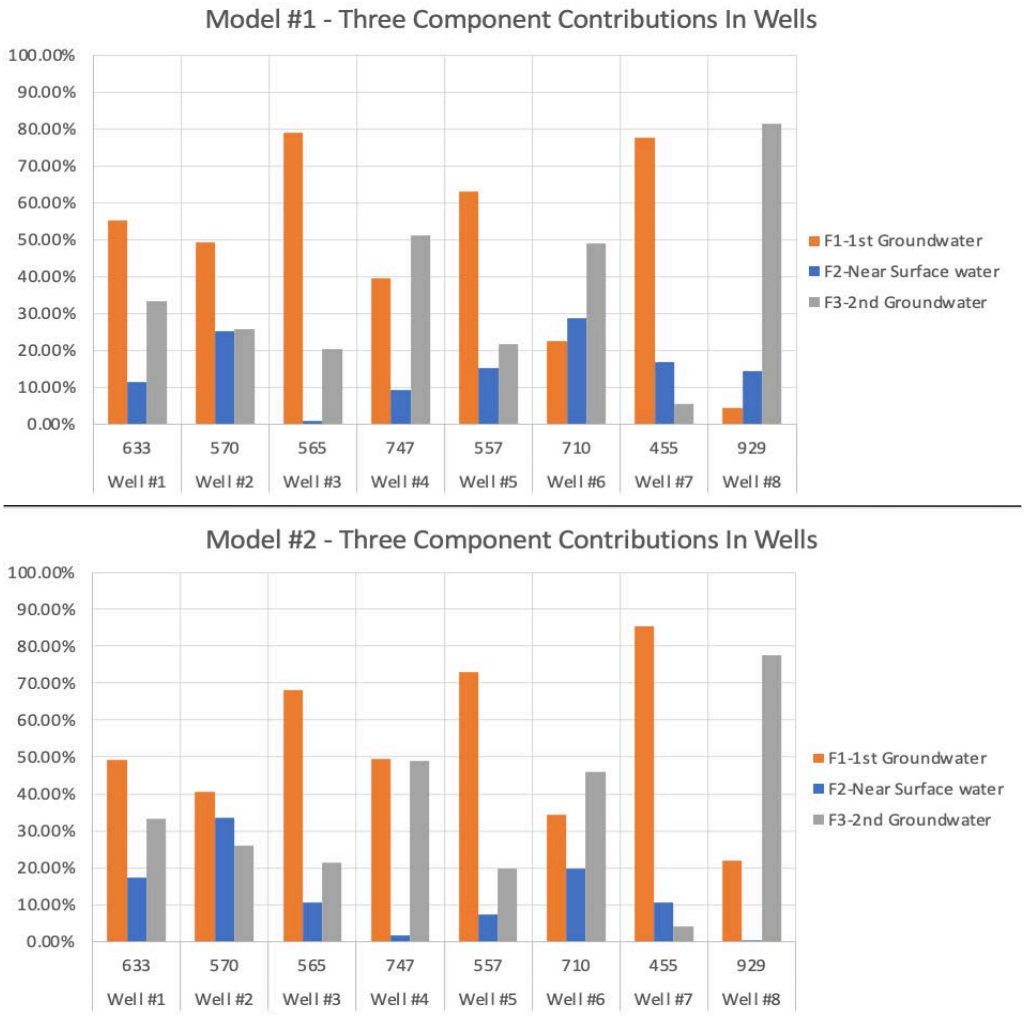

Figure 18: Percent contribution of the three sources in the well data from the two three-component models

3.7.1. Percent Contribution

The percent contribution of the three sources from model #1 and model #2 of water at different locations over time have similar spatial and temporal distributions (Figures 19 and 20). In May both models showed that all locations along the main channel had minimal contribution from 2nd groundwater, and had a significantly high contribution percentage from near surface water. Though there were slight differences between locations along the main channel and the models, generally there was a moderate contribution from the 1st groundwater in May. During

this time, both models showed that Ledford had significant contribution from the 2nd groundwater and Robb had a moderate contribution. Ledford and Robb both had moderate contribution from near surface water for may in model #1. However, in model #2, Robb had significant contribution from near surface water. In May both models showed a low percent contribution for 1st groundwater at Ledford and in model #1 moderate contribution at Robb. Model #1 does not have data for the beginning of May, while in model #2, Robb had a low percent contribution from the 1st groundwater on the beginning of May and moderate in the end of May.

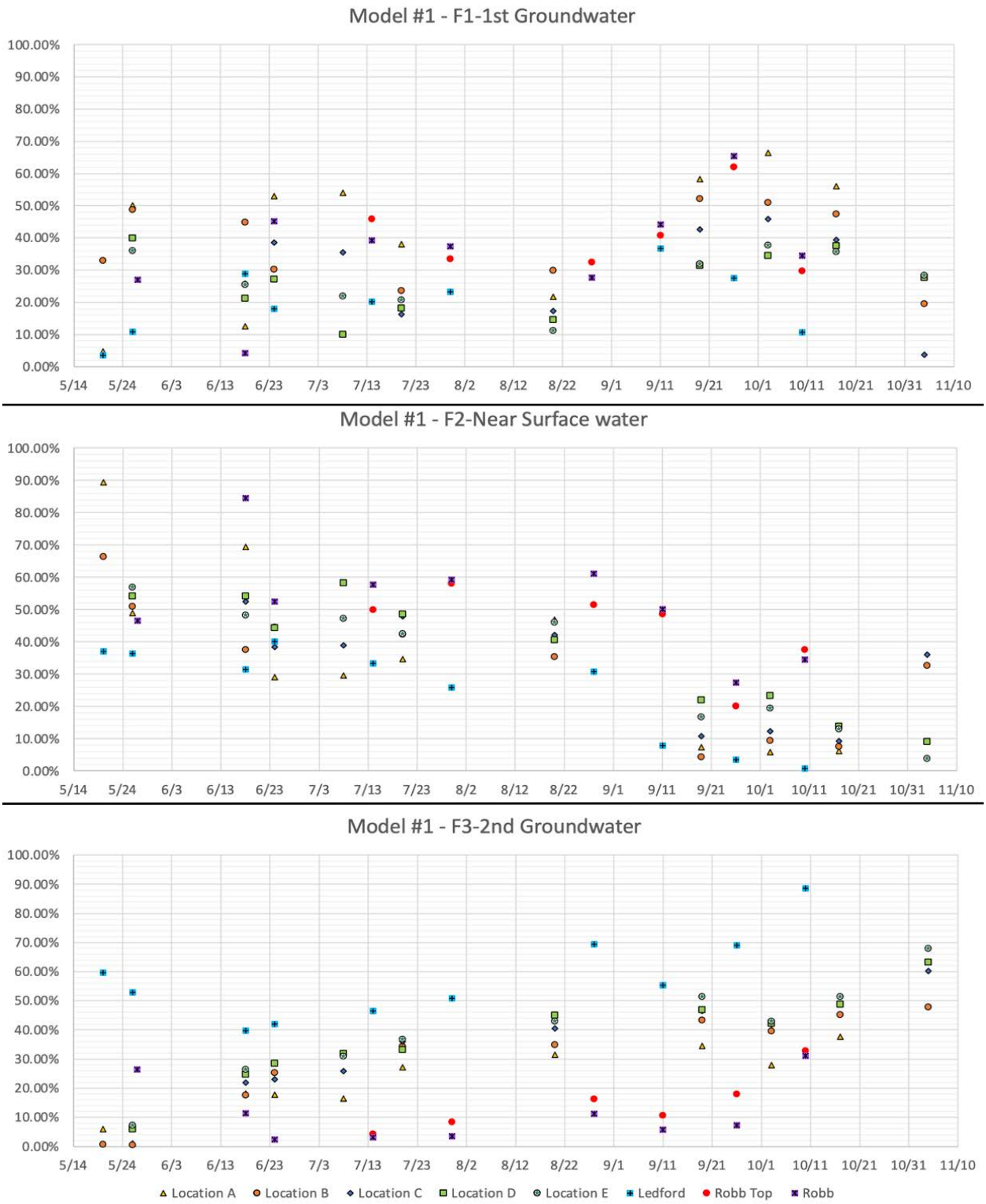

Figure 19:Percent contribution of the three sources from model #1 of water at the permanent monitoring locations over time.

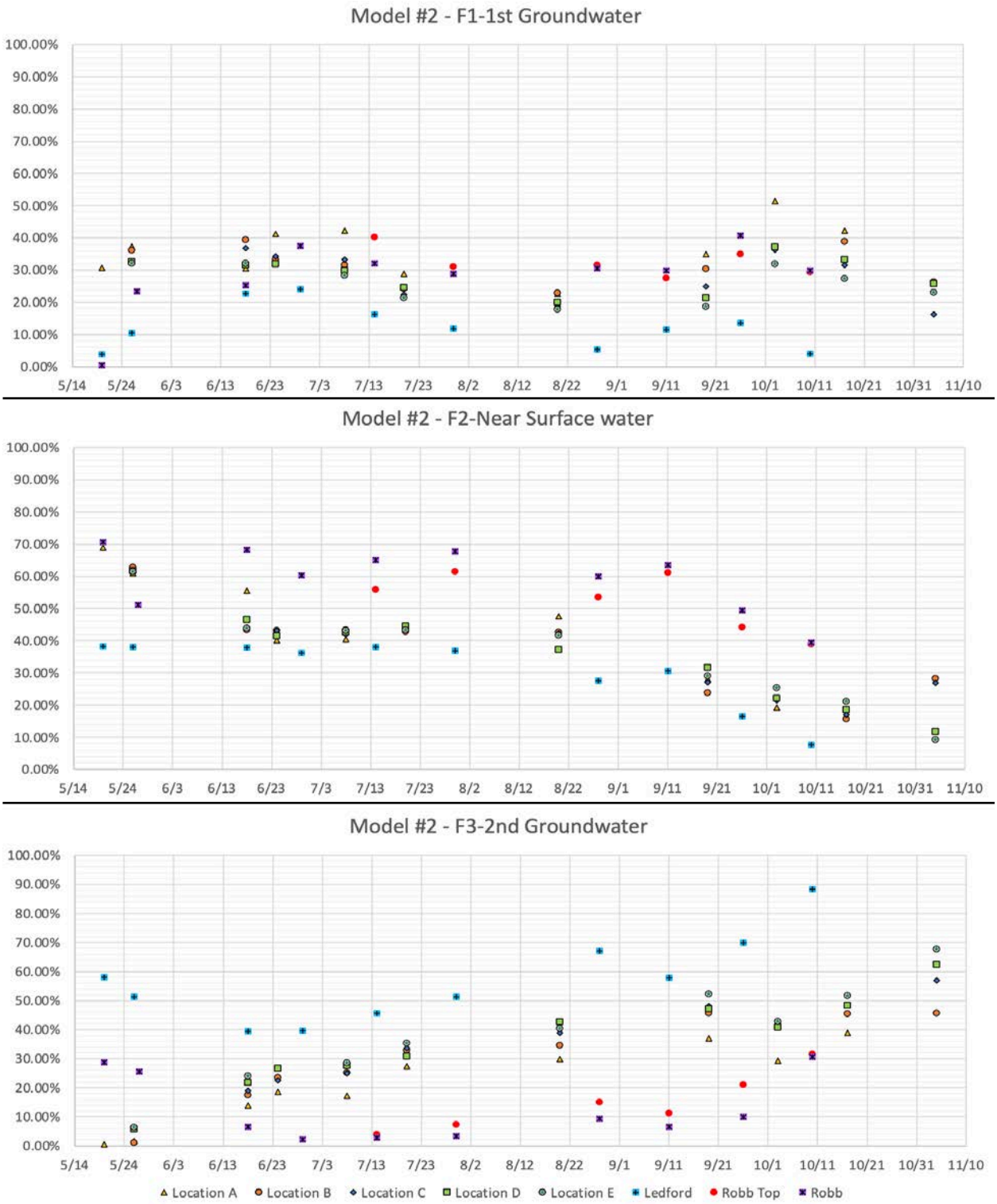

Figure 20: Percent contribution of the three sources from model #2 of water at the permanent monitoring locations over time.

3.7.1.1. 1st groundwater

Through November 4th the percent contribution fluctuated in both models (Figures 19 and 20). Locations A and B had higher percent contributions of the 1st groundwater than the other locations along the main channel with location A usually having the highest percent contribution. Both models show a rise in percent contribution of the 1st groundwater at all location in the beginning of July with a gradual decline until the end of August. From the end of August until the beginning of October there is another rise in percent contribution for the 1st groundwater at all locations. October through November showed a decrease in percent contribution for all locations in both models. In both rises of percent contribution of the 1st groundwater in July and October, the largest differences were seen in the upper most locations. The tributary percent contribution followed the same peaks at the beginning of July and October in both models. In both models, Ledford always had significantly lower percent contribution for the 1st groundwater than both of the Robb locations and though both locations on Robb were paired together, there wasn't one that was always a greater percentage than the other.

3.7.1.2. Near surface water

Through November 4th the percent contribution of near surface water remained mostly constant and only fluctuated slightly up until September when it decreased from moderate contribution to low contribution for both models (Figures 19 and 20). Model #1 has more separation between the contribution percentages within the main channel where model #2 generally grouped the main channel locations contributions from near surface water. Both models showed that in the end of the season, the upper most locations on the main channel had the lowest percent contribution from near surface water. Inversely the lower locations on the main channel had the highest percent contribution of near surface water within the main channel

clusters. In both models the Robb data had a higher contribution percentage than the main channel for near surface water while Ledford had significantly less contribution than the main channel and both locations on Robb. Both locations on Robb were paired together, however Robb Top usually had a lower contribution from near surface water.

3.7.1.3. 2nd groundwater

Through November 4th the percent contribution of the 2nd groundwater increased gradually until September when there was slight decrease followed by another gradual rise at all locations in both models (Figures 19 and 20). Both models showed that the upper most locations on the main channel had the lowest percent contribution from 2nd groundwater. Inversely the lower locations on the main channel had the highest percent contribution of the 2nd groundwater within the main channel clusters. In both models the Robb data had a much lower contribution percentage than the main channel for 2nd groundwater while Ledford had significantly higher contribution than the main channel and both locations on Robb. Both locations on Robb were paired together, however Robb Top usually had a higher contribution from 2nd groundwater.

3.7.2. Flowrate Component Contribution

The flowrate contribution by each of the three sources from model #1 and model #2 at the different locations over time have similar spatial and temporal distributions to each other and to the percent contribution of the three sources (Figures 19 - 22).

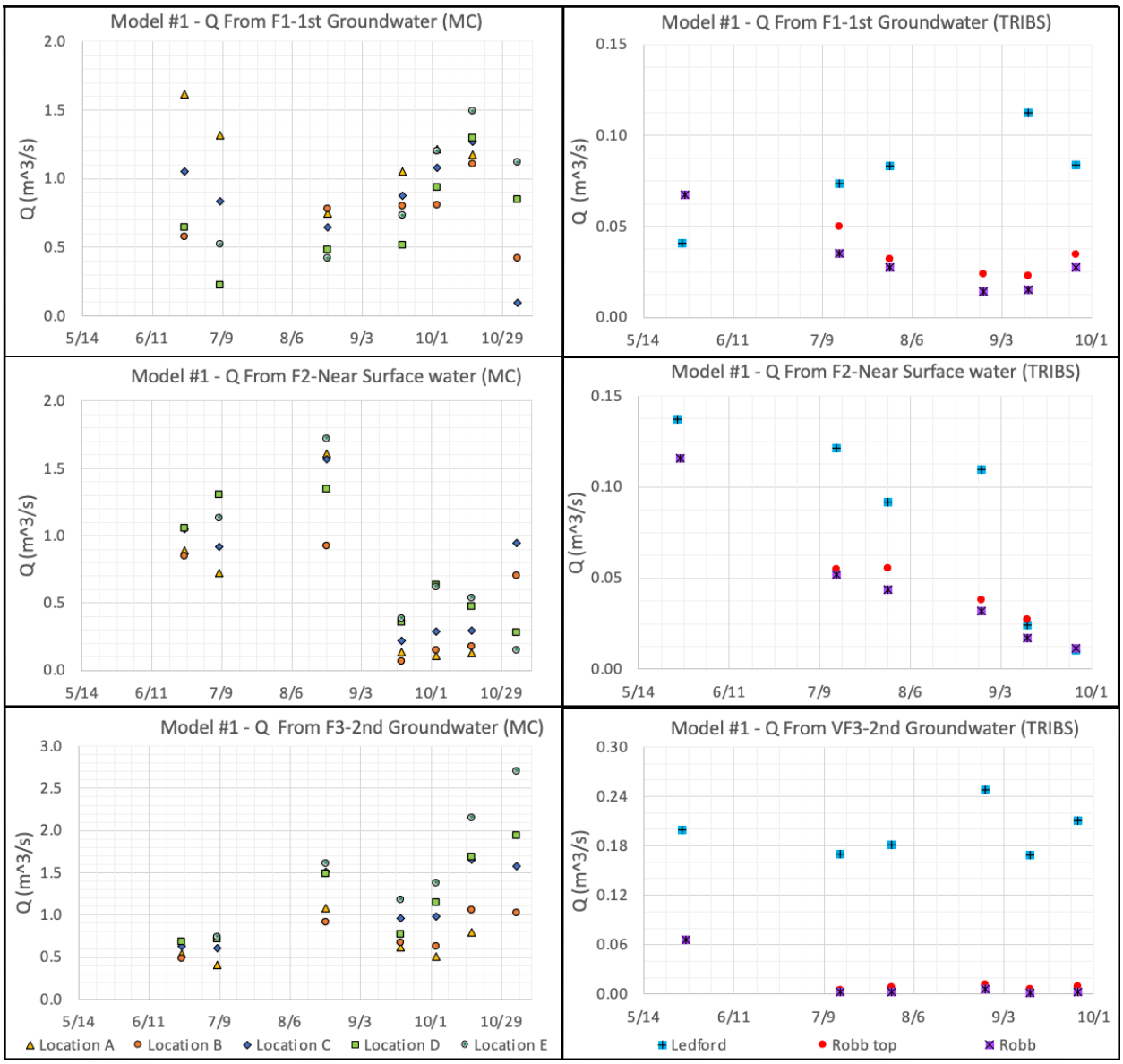

Figure 21: Flowrate per component for three-component mixing model #1

Description: Percentage contributions from model #1 were multiplied by the manually recorded flowrates at each of the permanent monitoring locations along the main channel (MC) and tributaries (TRIBS).

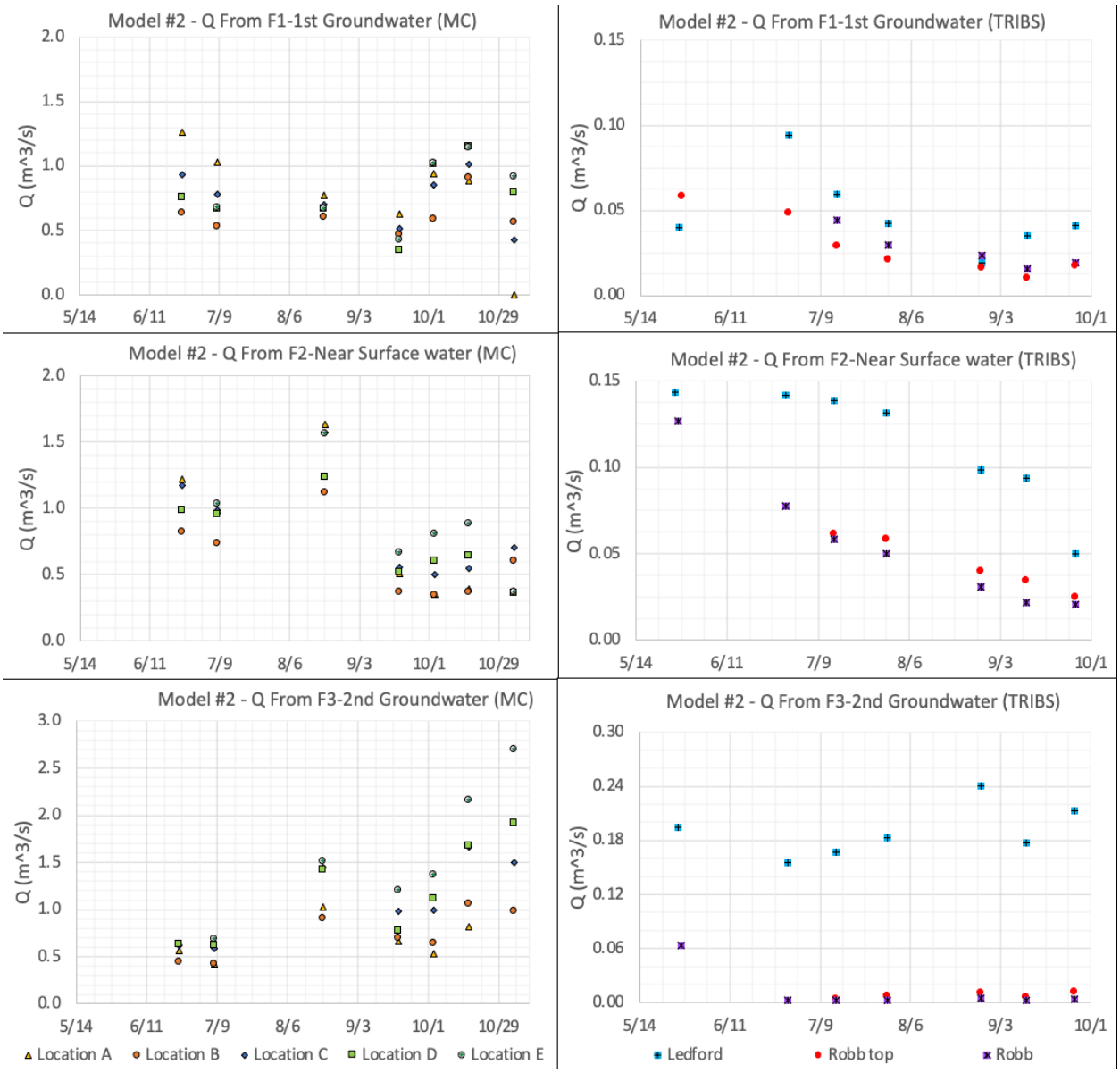

Figure 22: Flowrate per component for three-component mixing model #2

Description: Percentage contributions from model #2 were multiplied by the manually recorded flowrates at each of the permanent monitoring locations along the main channel (MC) and tributaries (TRIBS).

3.7.2.1. 1st groundwater

These models show a decreasing flowrate from the 1st groundwater in the upmost location A over the season, consistent flowrate at location B, and an increasing flowrate at all other main channel locations until November when the flowrate decreased at all locations

(Figures 21-22). Both models show a decreasing flowrate from the 1st groundwater in the end of June through the beginning of July. Location A had the highest flowrate from the 1st groundwater while location B had the lowest flowrate. In both models the flowrate at location B from the 1st groundwater remains fairly consistent with minor variations throughout the season other than one spike in flowrate in October and a slight decrease in November. In both models' locations D and E had a low the 1st groundwater flowrate in the beginning of the season and the highest flowrate from the 1st groundwater in the end of the season.

There is a slight discrepancy between the models for tributary flowrate from the 1st groundwater. In model #1 the flowrate from the 1st groundwater increases at Ledford throughout the season until late September when the flowrate decreases. However, in model #2 there is an increase in flowrate from May to July, a decrease from July until late August, and another increase from late august to October. In both models the flowrates from the 1st groundwater at both locations on Robb creek are clustered together and have a similar trend of slightly decreasing until September and then slightly increasing until November. The only difference between the two models for flowrates of the 1st groundwater on Robb creek is that model #1 has a higher flowrate at Robb top than Robb, while on model #2 the inverse is true.

3.7.2.2. Near surface water

The near surface water flowrates had discrepancies between the models, however had overall similar trends with an increase in late August for all locations, a decrease in flowrate from August to September, consistent flowrate from September to late October and a change in flowrate relationships in November (Figures 21-22). In June, for model #1 the Near surface water flowrates in the main channel were highest at location C and D while A and B were the lowest. In model #2 the highest flowrates in June were from location A and the lowest flowrate

was at location B. In both models the near surface water flowrate was generally the lowest at location B until November. However, in model #2 location A had a lower flowrate in October. In both models the near surface water flowrate was the highest in location D and E, the lowest in either location A and B from September through October. In November the flowrate from near surface water was the highest in location C followed by B, D and E in decreasing order.

The tributary near surface water flowrate has similar trends between models with only minor discrepancies of a decreasing flowrate from May through October for all locations. At Ledford the flowrate decreased gradually until September when the flowrate drastically decreased rapidly to equal the flowrate of both Robb locations. The Robb creek near surface water flowrates were grouped together and decreased rapidly until August and gradually decreased until October. In both models the flowrate from near surface water was higher at the upper location on Robb creek.

3.7.2.3. 2nd groundwater

The 2nd groundwater flowrates for the main channel are very similar between the models: The flowrates are mostly clustered together in June and beginning of July, begin to separate and increase in August, decrease in September and drastically rise through November. Anytime the flowrate of the 2nd groundwater increased the larger increases were seen at locations further downstream (Figures 21-22). Th roughout the data collection location D and E always has the highest flowrate and locations A or B had the lowest flowrate from 2nd groundwater.

The 2nd groundwater flowrates on the tributaries were comparable between the two models. Ledford’s 2nd groundwater flowrate was fairly consistent in both models with a slight decrease from May until mid-July, gradual increase from mid-July until late August, an increase

from late-August until early September, and an increase from early September until late September. In both models there is negligible flowrate from the 2nd groundwater in both locations on Robb creek except from the lower Robb location in May

3.8. Restoration

The area of gravel bars only was measured within the main channel and does not include bank armoring. There were 11 gravel bars observed from the 2022 drone imagery which totaled an area of 3,508 m^2 (Figures 23 - 24). There was also an observed five stretches of the river cutbank that brush bundles were used, this equated to a length of 522.4 m (Figures 23 - 24).

Figure 23:Restoration techniques brush bundles and plug and pond using gravel bars delineated from 2022 drone data overlayed on 2014 satellite data

Restoration techniques			
Brush bundles	Length (m)	Gravel Bar	Area (m^2)
1	161.0	1	214
2	82.5	2	205
3	85.0	3	294
4	73.9	4	197
5	120.0	5	570
		6	200
		7	222
		8	384
		9	778
		10	129
		11	315
Total	522.4	Total	3508.0

Figure 24: Delineated restoration technique values

Description: Distance along the main channel where brush bundles were used and area that gravel bars were used from Figure 23.

The restored area from 2022 show significantly more surface water area than in previous years. From 1995 until 2014 the main channel total surface water area increased (Figures 23-25). Over 10 years from 1995 until 2005 the main channel increased by 319 m^2, however from 2005 to 2011, over 6 years the main channel increased by 1,340 m^2 and from 2011 until 2014, over three years the main channel increased by 266 m^2 (Figure 23-25). From 2014 until 2022, after the restoration, the main channel area decreased by 1,591 m^2 which is 334 m^2 more than in 1995.

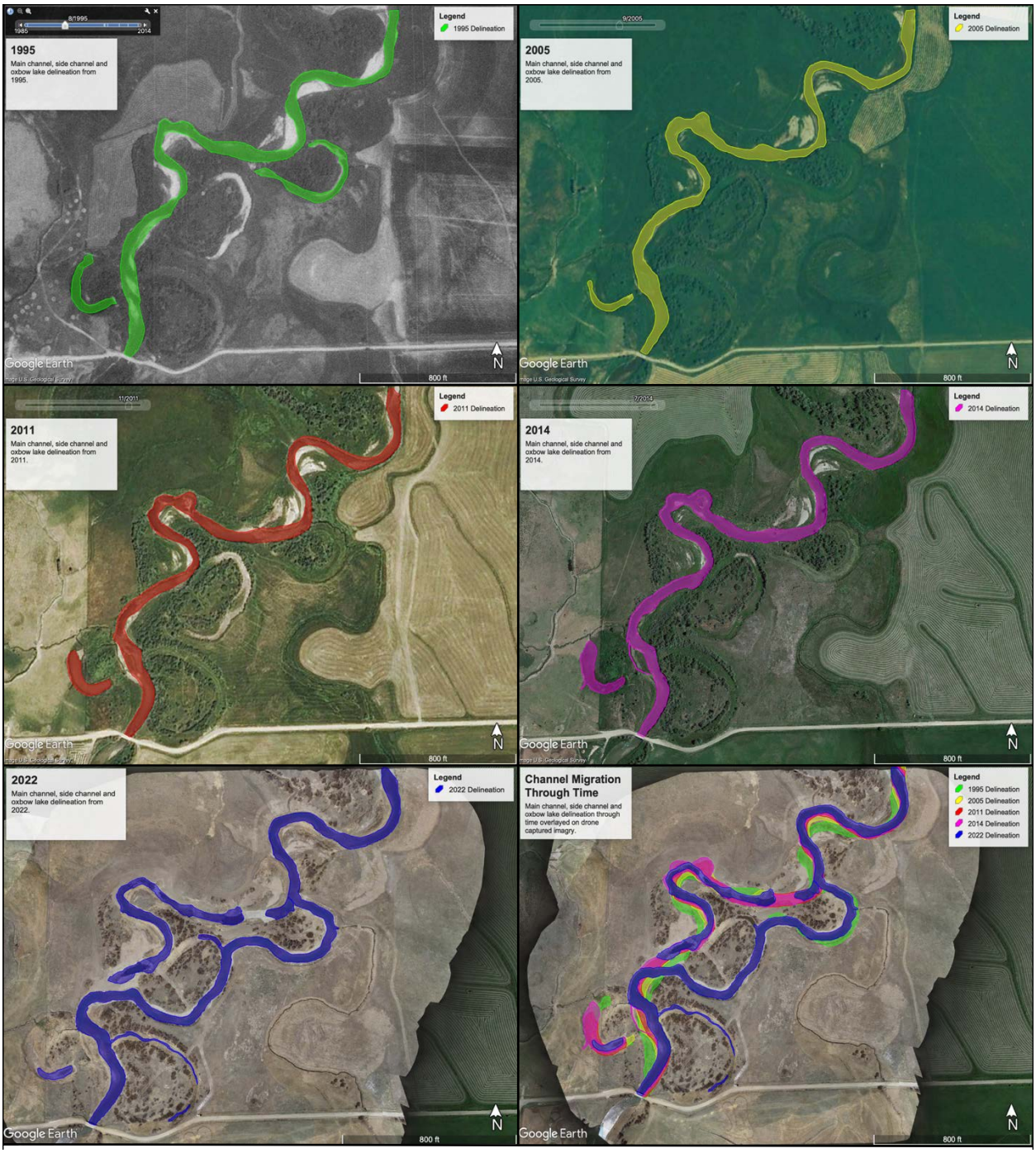

Figure 25:Surface water Delineation from historical satellite data from: August 1995, September 2005, November 2011, July 2014, and drone imagery from April 2022. The bottom right image compresses all of the delineations into one image overlayed on top of the 2022 Drone data.

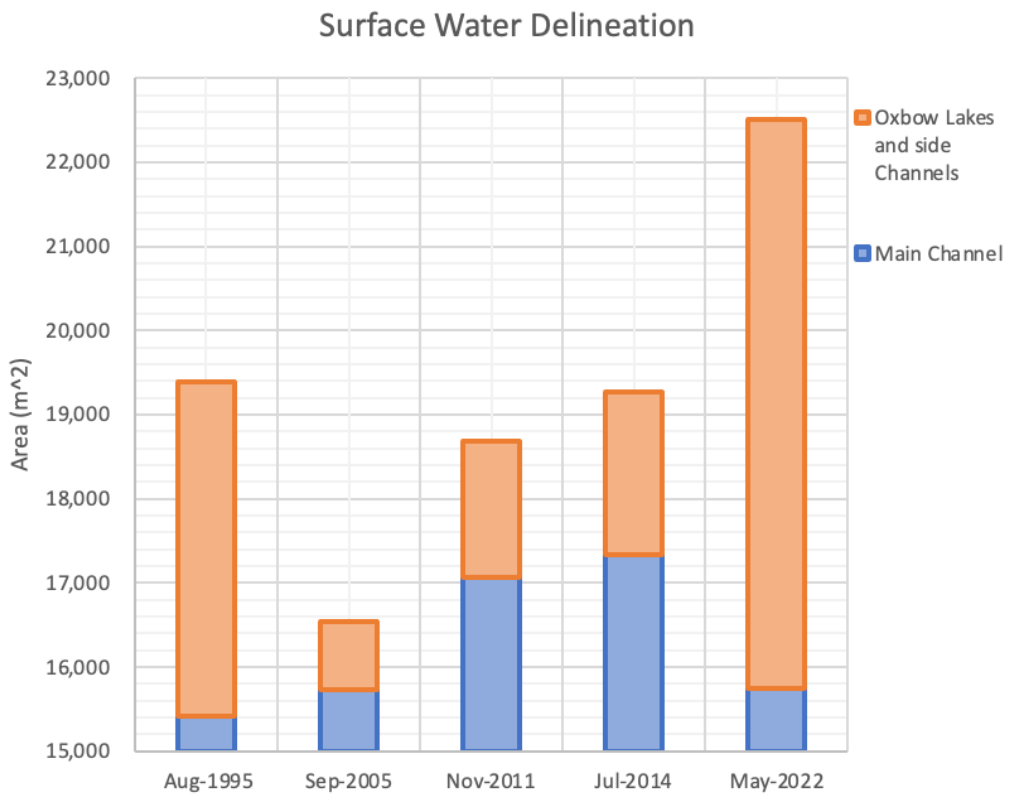

Figure 26: Surface water area delineation for both the main channels and a combined oxbow and side channels. Stacked values are the total surface water areas for each time period delineated

In both 1995 and 2014 there were two areas where surface water was present outside of the main channel. However, in both 2005 and 2011 there was only one area outside of the main channel with surface water. After the restoration in 2022 there was six delineations where there was surface water outside of the main channel (Figure 24-26). In 1995 and 2005 there was 3,981 m^2 and 818 m^2 respectively, of surface water in oxbow lakes and side channels. However, in 2011 and 2014 there was 1,620 m^2 and 1,942 m^2 respectively, of surface water in oxbow lakes and side channels. In 2022, after the restoration the surface water in oxbow lakes and side channels were 6,771 m^2, this is an increase of 4,829 m^2 from 2014. The combined area from all

surface water was 19,390 in 1995 and decreased by 2,844 m^2 by 2005 when the total surface water area was 16,546 m^2 (Figure 24-26). From 2005 until 2011 the total surface water area increased by 2,142 m^2 for a total of 18,688 m^2. However, while a significant amount of that increase came from the increase in surface water came from an increase in the main channel the side channels and oxbow lakes also increased by 802 m^2. From 2011 to 2014 there an increase in both main channel and side channel or oxbow lakes for a total of 19, 276 m^2 in 2014. There was a significant increase of 3,238 m^2 in total area from 2014 until post restoration in 2022, for a total of 22,514 m^2

4. Discussion

4.1. Temporal and Spatial Trends

The temporal and spatial trends of the upper Ruby River suggests that the flow regime is dominated by a source-sink relationship with groundwater. During snowmelt (May), location A had the highest flowrate, followed by locations C, E, D, then B in decreasing order (Figure 5 and 12). Both location B and D had less flowrate than the permanent monitoring location directly upstream because Peterson ditch and Pioneer ditch respectively remove water from the main channel. These ditches may aid in storing near surface water for late season flowrates. In June, the two-component mixing model shows both locations A and C had higher near surface water flowrates than locations B and D respectively (Figure 15). Over the course of the season, the flowrate of the upper locations began to drop such that all the instream flowrates were roughly equal except location B which was still significantly lower (Figure 5 and 12). At the end of the season, the flowrates follow a typical flow regime where flowrates at locations A-E increased with distance downstream (Figure 5 and 12).

The correlation of manual collection of flowrates to calculate continuous flowrates most likely causes errors in the projected continuous flowrates of locations C and D (Figure 11). The continuous flowrate data from this year can be compared to years following with functioning transducers to describe the periods of time with the most error. While this method may cause error, the manual flowrate data collection supports the spatial and temporal tends observed in the continuous flowrate data (Figure 5 and 12).

Temperature, SC and the stable water isotopes δD and δ18O can used as proxies for groundwater contribution. Groundwater is typically higher in SC, and around 10℃. At the beginning of the season, SC and temperature were both low with SC in the main channel being

around 400$\frac{\mu S}{cm}$ and temperature being <10℃ for the main channel (Figure 5), which suggests large contributions of fresh snowmelt and near surface water. A consistent pattern of increasing SC with distance downstream along the main channel was observed from May 27 through November 4 throughout the valley. The valley's temperature trend continued to decline from September 11 to November 4. However, the main channel temperature trends inverted such that the temperature generally decreased with progression downstream, suggesting an increase of groundwater percentage. By June 18th the temperature and SC increased such that a majority of the permanent monitoring locations temperatures were greater than 18.4°C and above 500 $\frac{\mu S}{cm}$. There was more of a notable change in δD than in $\delta O18$ from May to June however both isotopes became more depleted (Figure 9). This further suggests that at the beginning of the season a higher percentage of the water was from snowmelt, and is comparable to the SNOTEL data (Figure 2).

The end of the season is characterized by cold groundwater with a higher SC that dominates the system with less near surface water and more total contributions from groundwater even though total streamflow is lower. From June 18th until August 8th there was a decreasing trend in temperature and both stable water isotopes δD and δ18O with increasing trend in SC throughout the valley suggesting an increasing contribution of stored groundwater (Figures 5 and 8). When precipitation increased in October, SC still increased and temperature decreased. This suggests groundwater recharge, where an increase in precipitation would increase shallow groundwater return rates.

The surface water balance and load balance suggest a source sink relationship temporally and spatially with diches storing surface water for late season release. The surface water balance and load balance use flowrate and approximated load using a multiplier by SC to understand

reach by reach gains and losses. This model can be conducted under the assumption that a higher SC means a higher groundwater contribution. From the beginning of the data collection to the end of the season, both load balance and change in flow per reach increased. This suggests a source-sink relationship storing precipitation and releasing later in the season. From June until October the surface water balance and load balance show a loss in flowrate and load in reach A-B and C-D, which is most likely caused by the irrigation ditches pulling surface water out of the stream (Figure 13). Conversely, reach B-C and D-E were significantly higher in both surface water balance and load balance than the reaches directly above the respective reaches. This suggests that the surface water pulled out into the diches is coming back to the main channel as groundwater. Though surface water balance is a conventional method to estimate groundwater contribution and recharge, errors involved with the calculation of evaporation can lead to uncertainties (Haizhu et al. 2018).

The three-component mixing models and the two-component mixing model both represent the similar spatial and temporal trends along the main channel, having a source sink relationship of storing near surface water and releasing as groundwater. The source of the 1st groundwater contribution in the three-component mixing models will be discussed in more depth later, however for the system source-sink dynamic the 2nd groundwater contribution can be used synonymously with the groundwater in the two-component mixing model. The near surface water contributions are the same between the three-component and two component models. In November, the two-component mixing model shows an increase in flowrate from groundwater and a decrease in flowrate from near surface water with progression downstream (Figure 14). After September, both three-component mixing models also show an increase in percent contribution from 2nd groundwater component and a decrease in percent contribution from near

surface water in all MC locations (Figures 19 -20). This change from the beginning of the season to the end suggests a change from storing groundwater to releasing groundwater.

The synoptic flow data is the most spatially representative of the upper Ruby Valley and suggests that there are many gaining and loosing reaches as well as the importance of diches for storing surface water for late season return, however does not fully describe the temporal changes through the season. Though this was a surface water assessment, presumptions can be made for origins of water. The most upstream location used in the synoptic flow was 35 which had a flowrate of 2.030 $m^3/_S$ (Figures 6 - 7). Peterson dich represented by location 27, 1.6 km below location 35, removed 1.024 $m^3/_S$ leaving 1.032 $m^3/_S$ in the main channel at location 28. The secondary Ruby River channel observed contributing 0.208 $m^3/_S$ to the main channel just below Location B was not observed to have a source. This flowrate could be from un observed surface water or could be from groundwater return flow from Peterson ditch. However, if this is some return from Peterson ditch, there is a discrepancy of 0.816 $m^3/_S$, the majority of the flowrate at location 27. Though it is possible that this discrepancy is partially lost to evapotranspiration and evaporation, these affects would most likely be negligible compared to loss to groundwater. This discrepancy is most likely due to Peterson ditch is constantly losing to groundwater and is responsible for a majority of the 0.63 $m^3/_S$ of un accounted for flowrates within the main channel from locations 30, 25, 6, and 10.

The SC was not collected for the water samples from the synoptic flow, so these samples cannot be plotted against the two or three-component mixing models. All of the stable water isotopic compositions plot similar to the Butte MWL (Gammons et al 2006). However, while some of the well isotopic compositions were more depleted than the rest of the data, there was no spatial trend observed (Figure 8). The lack of spatial trend in isotopic compositions does not

mean there is not a spatial trend in groundwater influence, this simply means that the stable water isotopes alone do not fully describe these trends.

The temporal and spatial trends of the tributaries to upper Ruby River suggests that Ledford creek is a spring fed tributary and that Robb creek is a surface water fed tributary. Ledford creek had consistently the highest SC and lower temperatures, especially after snowmelt had ended in June and before the snow came back in September. Ledford also had consistent flowrates that weren't as impacted by storm events (Figure 12). This could suggest that Ledford has a dynamic better suited for storing surface water and releasing over time. Conversely, Robb creek consistently had low SC and high temperatures until October, which means that this is most likely a melt dominated tributary. Robb creek is also losing water to the groundwater from upper location to bottom location as evident by higher SC and flowrate at the upper location and slightly lower temp at the upper location. The temperature could be lower because of a reduced time in stream from snowmelt or source (Figure 5). Temperature, SC and Stable water isotopes can change with distance traveled and contribution from other sources so a direct comparison for temperature, SC and water isotopes without more context do not provide a complete understanding of the system dynamic.

The two and three component mixing models both suggest that Ledford is a spring fed or groundwater dominated tributary, while both locations on Robb Creek are surface water dominated. The source of the 1st groundwater contribution in the three-component mixing models will once again be discussed in more detail later. However, for the system source-sink dynamic, the 2nd groundwater contribution in the three-component mixing models can be used interchangeably with the groundwater in the two-component mixing model. Ledford consistently had the lowest percentage of near surface water in both of the two and three-component mixing

models and the highest percentage of groundwater or 2nd groundwater contribution in the three-component mixing model (Figure 14, 19 and 20). Robb Creek at both locations had the highest percent contribution from near surface water and the lowest percent of groundwater/ 2nd groundwater for a majority of the data collection (Figure 14, 19 and 20).

4.2. Three-Component System Dynamic

The three-component mixing models suggest that there are two sources of groundwater and a near surface water component that are mixing. However, while the source of the groundwater components can be suggested, there is no clear evidence to prove the source of the two groundwater components.

The well data generally plots along the F1 to F3 mixing line suggesting that there are two sources of ground water (Figures 17 -18). If there was only a single source of groundwater, the well data would most likely be isolated to a single component. In comparison to the 2nd groundwater component, the 1st groundwater component has a much lower SC and depleted of both stable water isotopes δD and δ18O. Meaning that there is a groundwater component, F1-1st groundwater, slightly higher in SC and very isotopically depleted in comparison to the near surface water. There is also a groundwater component, F3-2nd groundwater with a very high in SC and slightly depleted isotopically in comparison to the near surface water.

The three-component mixing models suggest that SC is not fully representative of the groundwater contribution (Figure 17). This means that the two-component mixing model and the load balance is slightly oversimplified and does not represent the full complexity of the system dynamic. When comparing the composition of the well data for both of the three-component mixing models with the well data for the two-component mixing model there are some discrepancies that also suggest that the two-component mixing model is over simplified

(Figure 16 and 18). The majority of the well data from the two-component mixing model had a majority contribution from near surface water while in both three-component mixing models the composition of all of the well water is primarily of either F1-1st groundwater or F3-2nd groundwater.

4.2.1. Model validation

Both of the three-component models did not numerically validate using the EMMA validation (Figure 27). Model #1 had an R^2 of 0.4804 while model #2 had an R^2 of 0.6583. The three-component mixing model shows that a majority of the samples taken from the surface are more enriched in δD than in $\delta 18O$ in comparison to the well data, however still plots the GMWL. Though the models could not be numerically validated they can be conceptually validated with similar spatial and temporal trends from the data (Figures 17-22). Comparing the results for each data point between the models, there is a R^2 value of 0.7878 for all of the data (Figure 28). Breaking down each data point by component and comparing the models for F1, F2, and F3 there was a R^2 value of 0.592, 0.7861, and 0.9923 respectively. This suggests that components of the data can be more validated than others. F3-2nd groundwater is validated while there are some possible errors in F2-near surface water and the largest source of error between the two models is F1-1st groundwater. The three-component mixing model suggests a complex system and that there are most likely more extreme endmembers reflecting our representation of the three components. Well drilling or other exploration may be needed to more accurately describe the endmembers. However, the spatial and temporal patterns seem to qualitatively reflect the patterns for a source sink relationship of storing near surface water and releasing as groundwater later in the year.

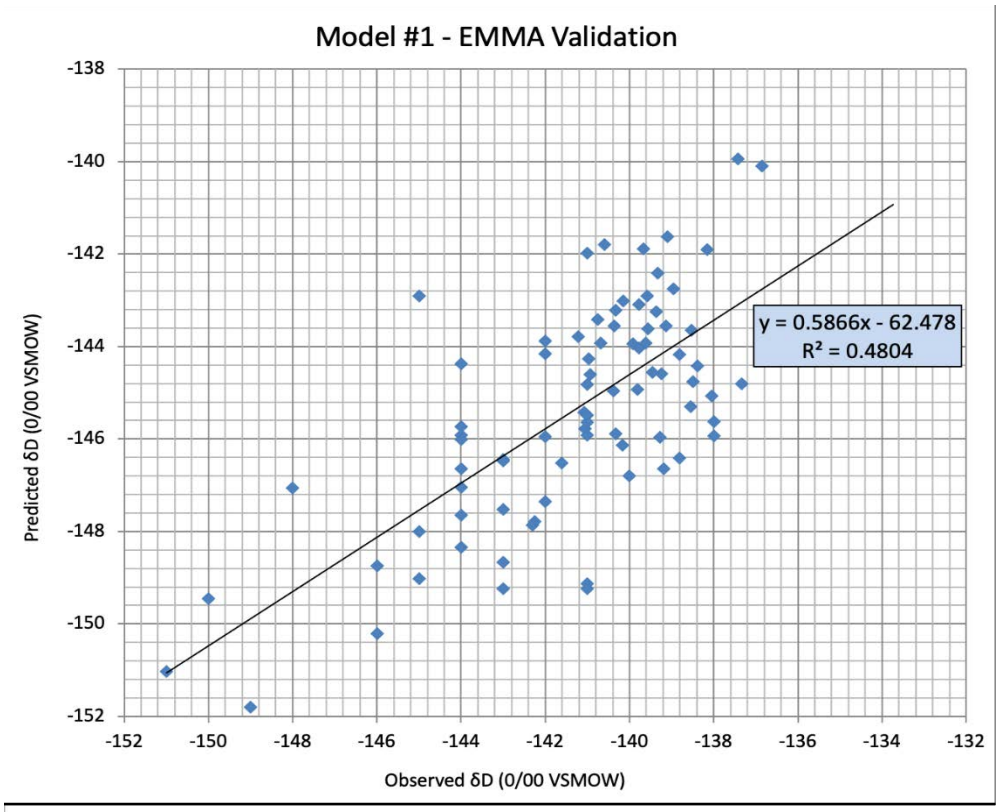

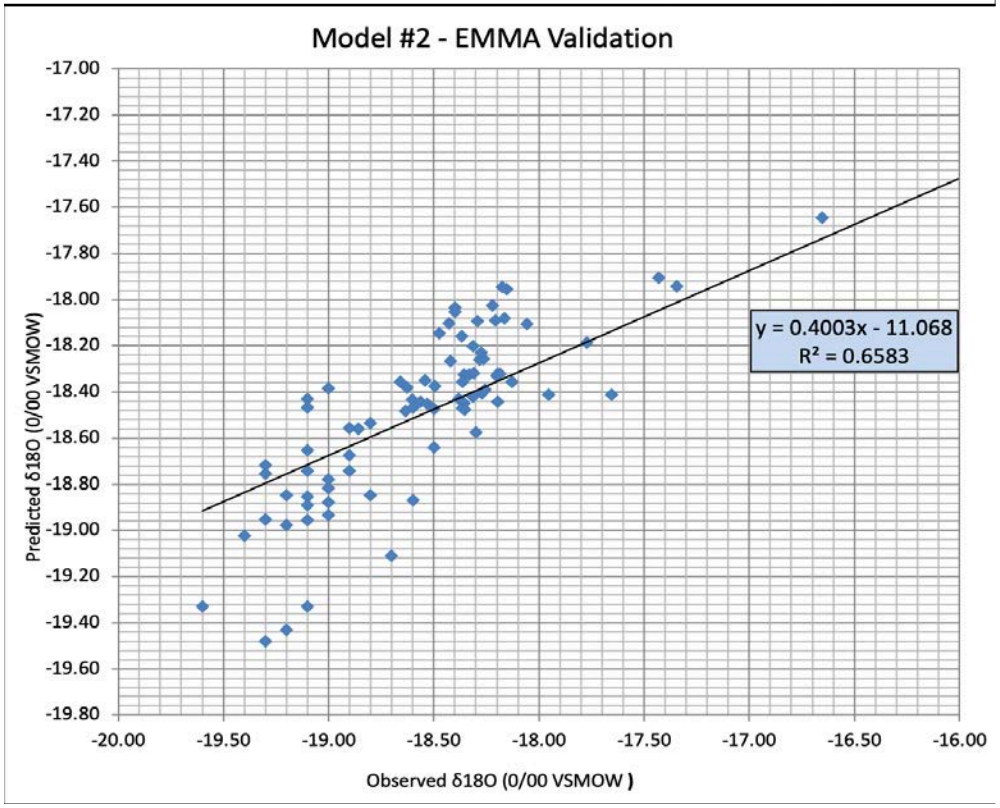

Figure 27: EMMA Validation for both models

Description: Relationship between observed data and predicted values for a geochemical parameter not used in the mixing analysis. The predicted values were calculated by multiplying the fractional percentage for all data by end member of the other model (Table 1).

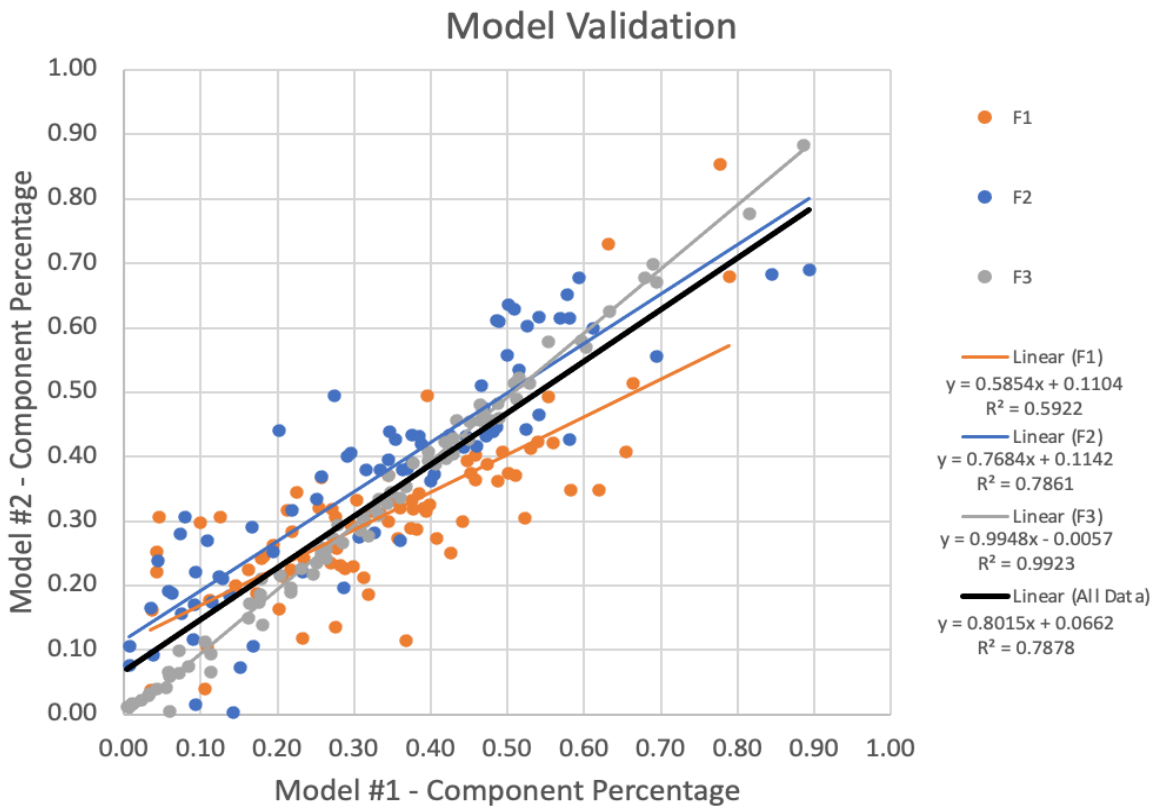

Figure 28: Percent contribution for each of the three components for model #1 vs. the Percent contribution for each of the three components for model #2

4.3. Potential Sources of Groundwater

The source of the two groundwater components could be associated with a change in lithology Quaternary Alluvium and Tertiary sediments (Figure 1 and 3). However, in this study the change in lithology does not correspond directly with observed composition from the tributaries or well water. In both three-component models, Ledford was significantly higher in the F3-2nd groundwater while both Robb creek locations had significantly more F1-1st groundwater by volume and percentage (Figures 19-21). The location of sample collection compared to the geologic map would suggest both locations would be Tertiary sediments.

The change in composition of groundwater could be due to physical groundwater gradient more than lithology. Differences in composition from bench groundwater and valley groundwater have been observed in other studies. However, here the topography driving change in composition also does not corelate with locations of tributary data or with well data. Though because of the lack of information provided for total well depths, there may be a difference in composition due to the well water accessing different sources of water based on depth.

The four mountain ranges that surrounded the upper Ruby valley could possibly be producing different compositions of groundwater. The Snowcrest range to the south southwest, Gravelly range to the southeast, the Greenhorn range to the northeast and the Ruby range to the northwest. While this study does not have sufficient data to fully determine this, it is unlikely based on tributary data. Both Robb creek and Ledford creek are creeks attributed to surface water and groundwater from the Snowcrest mountain range. These correlations are not validated and cannot be used as causation for composition variation.

The F1-1st groundwater and F3-2nd groundwater could come from different horizontal layering. The horizontal hydraulic conductivity and permeability is typically greater than the vertical conductivity and permeability in most sediments (Hem, 1985). Because of this, Groundwater also typically does not mix very well and could be the reason there are two groundwater signatures. In this scenario, it is more likely that F1-1st groundwater has a lower residence time, and probably more local flowpaths (Toth, 1963) because it has a lower SC, suggesting a shorter amount of time in contact with near surface rock and minerals (Hem, 1985). Though the higher SC in F1-groundwater than F2-Near surface water could be partially associated with solutes directly applied in agriculture (Hem, 1985). Conversely, F3-2nd groundwater most likely has a higher residence time as it has a higher SC.

It is likely that F1-1st groundwater was from irrigation return flow from ditches or from groundwater that has been pumped for irrigation. Irrigation can be significant recharge to groundwater or to streams (Hem, 1985). F1-1st groundwater is more isotopically depleted than both F2- near surface water and F3-2nd groundwater, which could suggest more evaporation. The well data being more depleted in δD and $\delta 18O$ than the instream isotopic distribution supports F1-1st groundwater was from irrigation return flow (Figure 8). As meteoric waters evaporate, in diverted water, the isotopic composition typically becomes less depleted (Jasechko, 2019. e.g., Williams & Rodoni, 1997). This also may justify some of the complexity or error observed in the three-component mixing models especially between F1 and F2 as these are often mixing and separating at multiple locations along the Ruby (Figures 21-22). This supports F1-1st groundwater and F3-2nd groundwater originating from different horizontal layering. Where the upper groundwater source, F1-1st groundwater, is from irrigation return and the deeper groundwater source is the F3-2nd groundwater. There was a rise in percent contribution of the F1-1st groundwater at all location in the beginning of July with a gradual decline until the end of August (Figures 19-22). From June 18th until August 8th there was a trend of increasing temperature with distance downstream along the main channel which could be attributed to irrigation return heating up with progression downstream (Figure 5). The F1-1st groundwater contribution was the only component in the three-component mixing models that was higher at the lower Robb location.

There are, however some other possibilities as to the process controlling the isotopic depletion in both groundwater sources. Due to the high topographic relief of the upper Ruby valley, it is likely that groundwater is recharged from higher elevations, mountain block recharge, that would be more isotopically depleted (Jasechko, 2019). This is most likely the case

of the depletion from F2-near surface water to F3-2nd groundwater. However, this does not describe the separation of two groundwater sources or exclude irrigation return as a source for F1-1st groundwater.

Stable water isotope compositions have been observed to fluctuate seasonally where precipitation from the wet season is typically more depleted and during the dry season. This could also suggest that the groundwater contributions are more dependent on the wet season recharge (Yeh, et al. 2014). This study does not directly observe precipitation and therefore some error may be observed on using isotopic trends in relation to meteoric water.

4.4. Restoration

Fish habitat encompasses a majority of secondary drivers for restoration, bringing economic and cultural benefits to the upper Ruby River (Galatowitsch, 2012). Primary drivers for restoration are mostly land conversion from the development of the land for farming practices and beaver trapping. The ecological stressors include a shallow main channel depth, over steepened banks, decreased stream cover and warm stream temperatures. These ecological stressors in the upper Ruby River have most likely caused the affected ecological attributes of decreased biodiversity, ecosystem stability and ecosystem function as a causation from the observed stressors. Although a thorough ecological analysis has yet to be conducted on the upper Ruby River. The major purpose for restoration is to enhance the ecosystem functionality for physical properties such as nutrient cycling, biological structure and mainly material movement within the system which include geomorphological changes and natural water regimes.

Beavers are a keystone species have been fundamental in improving river ecosystems. Beaver dams decrease stream velocity and connect the stream better to the floodplain. This creates a source/sink relationship for water and nutrient storage (Wegener et al., 2017). During

high-flows dams sink nutrients and water, reducing the volume moving downstream. During low-flows, beaver dams are a source for water and nutrients, releasing it downstream. A loss of beavers from an area can lead to increased stream velocities, channel intrenchment, and decreased riparian wetland habitat which support more complex ecosystems (Marston, 1994). Riparian vegetation in turn provides shade for the stream and reduces stream temperatures which further degrade the ecosystem (Beschta, 1997). Beaver have been and still are trapped out of some locations in the upper Ruby Valley.

The goal of the Plug and Pond system with brush bundles used as bank armoring installed on the upper Ruby River is to store surface water for late season flow. This is intended to replace some of the ecosystem services that beaver provide. The areal analysis of surface water suggests that there is a shift in surface water into side channels and oxbow lakes and an increase in total surface water. The increase in total surface water could be attributed to a rise in ground water and the transition from in the main channel into side channels and oxbow lakes would most likely benefit late season flowrates. Rising the water table especially during sensitive times would greatly benefit fish populations. The gravel bars most likely decrease the stream velocity and the stream power. A combination of decreased stream power and stabilized cutbanks with brush bundles will most likely lead to a decrease in channel incision. Based on the areal delineation of surface water over time, and restoration techniques, this restoration will benefit the ecosystem for a long period of time.

The hydrological analysis suggests the Plug and Pond system with brush bundles installed on the upper Ruby River will store surface water for late season flow. These restoration techniques slow stream velocities and have been observed to store water in side channels and oxbow lakes (Figure 25). As the F1-1st groundwater source observed in the three- component

mixing model is likely due to irrigation return, it is likely that the plug and pond system will store the F2-near surface water for late season signatures of the F1-1st groundwater component similar to the irrigation diches. This source sink dynamic mimics beaver activities while not disrupting fish passages like beavers can.

The data from this study suggest that Ledford a tributary that is groundwater dominated with high contributions of groundwater in Load balance, two-component, and in both three-component models. This tributary has consistent lower temperature and higher flowrates. This tributary needs to be preserved and not restored as it is functioning and healthy from a hydrologic perspective. Robb creek is a surface water dominated tributary and is hydrologically impacted. Hydrologic and ecological restoration such as plug and pond or beaver mimicry structures should be completed on Robb creek to store surface water for late season flows.

Possible errors in the surface water area delineations are that the satellite data came from multiple times of the year where seasonal flowrates fluctuate. This could be corrected by taking data multiple times throughout a year and comparing on a month-to-month basis, or comparing similar trend in the USGS flowrates over the years. Another, possible source of error is the poor resolution of historical data, this would lead to inaccurate delineations. This data is significant as it uses drone data in an ecological assessment and in Restoration. Initially the idea for this project was to delineate plant species and distance from river or to use the Digital Elevation Model (DEM) collected. The data collected from drones is significantly faster than differentiate species on the ground. These are still valid concepts for projects and justify more drone work to be used in restoration.

5. Conclusion

This study was designed to analyze the complex hydrology of the upper Ruby River valley on a large scale using a multitude of hydrological analysis, and models using tracer techniques. The temporal and spatial trends of the upper Ruby River suggests that the flow regime is dominated by a source-sink relationship with groundwater. Flowrate, temperature, SC, δD and $\delta 18O$ were all collected periodically in stream at the 5 main channel and 3 tributary permanent monitoring locations for general spatial and temporal analysis of the upper Ruby valley from May 27th to November 11th. This suggests a seasonal source sink relationship with part of the year

A single synoptic flow event in the end of the season was utilized for a more in-depth analysis of spatial variation within the complex watershed. The Synoptic flow event suggests many gaining and losing reaches along the main channel. Measured ditches and tributaries contributed 0.972 $m^3/_S$ to the main channel flow rate, whereas ditches removed 1.654 (m3)s from the main channel. this suggests a loss to evapotranspiration or to groundwater, though not all of the river's ditches and tributaries along its 43.5 km length are taken into account.

The stable water isotopes collected from the permanent monitoring locations, the synoptic flow event, and 8 well water collections were plotted against Butte MWL and the GMWL. The bulk of the isotopic compositions of river samples are enriched when compared to the GMWL and depleted when compared to the Butte MWL. The well water is also more depleted than the majority of the river samples. This may be because of differing evaporation rates from irrigation ditches evaporating and recharging groundwater. If this process is evaporation driven, the Butte MWL is less representative of the upper Ruby River valley than the

GMWL. In Bailey et al. 2022, a local meteoric water line was established for a small reach along greenhorn, a tributary to the Ruby River from precipitation collected. While this study is not fully representative of the entire upper Ruby Valley there are similar evaporation trends for the majority of the soil and groundwater samples (Bailey et al. 2022).

In Situ pressure transducers were installed in stilling wells at the permanent monitoring locations. Creating a rating curve from the flowrates a continuous flowrate could be made for the permanent monitoring locations giving very detailed temporal variations. The Transducer data was not recovered for locations C and D. A correlation was made between manual flowrates from Locations B to C and from E to D. There most likely has some error attributed to this methodology. However, this type of approximation could be useful in filling in missing information of future studies if this methodology could be validated. This could be done by comparing continuous flowrates of multiple years at the same locations to years with some approximated locations.

Multiple models were constructed using the parameters: flowrate, SC, δD and $\delta 18O$ to analyze source of water compositions. Surface water and Load balance models were constructed from SC and flowrate. Load balance model used SC to approximate a mass per time of solutes to estimate groundwater. Two-component mixing model used SC as a tracer to identify groundwater vs near surface water constituents. The spatial and temporal trends of the surface water balance, load balance, and two component mixing model suggest a source-sink dynamic producing more groundwater later in the season and further downstream.

Two three-component mixing models were constructed using $\delta 18O$ vs. SC for the first model and δD vs. SC for the second model. Though nether three component mixing model could be numerically validated they are conceptually validated through similar spatial and temporal

trends. This most likely means that the load balance and two component mixing models are over simplified for the upper ruby river. This also suggests that a major source of water is from irrigation return or bench groundwater. The isotopic distribution of the samples collected may also suggest that the Butte MWL does not fully represent the upper Ruby River valley.

Aerial imagery from an RTK drone flight and historical satellite imagery was used to delineate surface water over time and compare post restoration for a restored reach on the Ruby River. This study establishes regional baseline hydrological processes and discusses impacts of ecological restoration on hydrology for the semiarid upper Ruby River valley. However, one of the major limitations is that the restoration drone data is only encompassing of part of a single year and does not fully describe climactic changes. Further studies using isotopic composition drift due to restoration and surface water storage should be completed in this area to assess if the evapotranspiration is outweighed by the groundwater recharge. Additionally, mountain groundwater should be collected to asses mountain block recharge to the groundwater for the upper Ruby River valley.

There is an increase in total surface area of oxbow lakes and side channels which could be a result of a raised water table. The hydrological analysis suggests the Plug and Pond system with brush bundles installed on the upper Ruby River could store surface water for late season flow. Restoration will store the F2-near surface water from the three-component mixing model in side channels and oxbow lakes for late season evaporated signatures of the F1-1st groundwater.

This study suggests that Ledford creek is spring fed while Robb Creek is surface water dominated and hydrologically impaired. Ledford creek should be preserved and not restored as it is functioning and healthy from a hydrologic perspective. However, on Robb Creek hydrologic

and ecological restoration such as plug and pond or beaver mimicry structures should be completed on to store surface water for late season flows.

6. References Cited

Bailey, K., Korb, N., Kruse, C., Harris, S., & Hu, J. (2022). Water use strategies between two co-occurring woody species in a riparian area: Naturally occurring willow, *salix exigua* , and expanding juniper, *juniperus scopulorum* , in Central Montana. *Ecohydrology*, *15*(3). https://doi.org/10.1002/eco.2402

Beschta, R. L. (1997). Riparian shade and stream temperature; an alternative perspective. Rangelands, 19(2), 25-28

Boyd, K., and S. Gillian 2018. Ruby River at RVHA Geomorphic Evolution Stream and Riparian Restoration Alternatives.

Bufe, A., Turowski, J. M., Burbank, D. W., Paola, C., Wickert, A. D., & Tofelde, S. (2019). Controls on the lateral channel-migration rate of braided channel systems in coarse non-cohesive sediment. *Earth Surface Processes and Landforms*, *44*(14), 2823–2836. https://doi.org/10.1002/esp.4710

Constantz, J. (2008). Heat as a tracer to determine streambed water exchanges. *Water Resources Research*, *44*(4). https://doi.org/10.1029/2008wr006996

Frisbee, M. D., Phillips, F. M., Campbell, A. R., Liu, F., & Sanchez, S. A. (2011). Streamflow generation in a large, alpine watershed in the southern Rocky Mountains of Colorado: Is streamflow generation simply the aggregation of Hillslope runoff responses? *Water Resources Research*, *47*(6). https://doi.org/10.1029/2010wr009391

Galatowitsch, S. M. (2012). *Ecological restoration* (p. 630). Sunderland: Sinauer associates.

Gammons, C. H., Poulson, S. R., Pellicori, D. A., Reed, P. J., Roesler, A. J., & Petrescu, E. M. (2006). The hydrogen and oxygen isotopic composition of precipitation, evaporated mine water, and river water in Montana, USA. *Journal of Hydrology*, *328*(1-2), 319–330. https://doi.org/10.1016/j.jhydrol.2005.12.005

Hem, J. D. (1982). Conductance: A collective measure of dissolved ions. *Inorganic Species*, 137–161. https://doi.org/10.1016/b978-0-12-498301-4.50009-8

Hem, J. D. (1985). *Study and interpretation of the chemical characteristics of natural water*. Dept. of the Interior, U.S. Geological Survey.

Jasechko, S. (2019). Global isotope hydrogeology—review. *Reviews of Geophysics*, *57*(3), 835–965. https://doi.org/10.1029/2018rg000627

Koeniger, P., Gaj, M., Beyer, M., & Himmelsbach, T. (2016). Review on soil water isotope-based groundwater recharge estimations. *Hydrological Processes*, *30*(16), 2817–2834. https://doi.org/10.1002/hyp.10775

Kondolf, G. M., Boulton, A. J., O'Daniel, S., Poole, G. C., Rahel, F. J., Stanley, E. H., Wohl, E., Bång, A., Carlstrom, J., Cristoni, C., Huber, H., Koljonen, S., Louhi, P., & Nakamura, K. (2006). Process-based Ecological River Restoration: Visualizing three-dimensional connectivity and dynamic vectors to recover lost linkages. *Ecology and Society*, *11*(2). https://doi.org/10.5751/es-01747-110205

Marston, R. A. (1994). River entrenchment in small mountain valleys of the Western USA : Influence of Beaver, grazing and clearcut logging / l'incision des cours d'eau dans les petites Vallées Montagnardes de l'Ouest Américain : L'influence des castors, Du Pâturage et des coupes forestières à blanc. *Revue De Géographie De Lyon*, *69*(1), 11–15. https://doi.org/10.3406/geoca.1994.4232

Muangthong, S., & Shrestha, S. (2015). Assessment of surface water quality using multivariate statistical techniques: Case study of the Nampong River and Songkhram River, Thailand. *Environmental Monitoring and Assessment*, *187*(9). https://doi.org/10.1007/s10661-015-4774-1

Naumburg, E., Mata-gonzalez, R., Hunter, R. G., Mclendon, T., & Martin, D. W. (2005). Phreatophytic vegetation and groundwater fluctuations: A review of current research and application of ecosystem response modeling with an emphasis on Great Basin vegetation. *Environmental Management*, *35*(6), 726–740. https://doi.org/10.1007/s00267-004-0194-7

Pan, B., Yuan, J., Zhang, X., Wang, Z., Chen, J., Lu, J., Yang, W., Li, Z., Zhao, N., & Xu, M. (2016). A review of ecological restoration techniques in fluvial rivers. *International Journal of Sediment Research*, *31*(2), 110–119. https://doi.org/10.1016/j.ijsrc.2016.03.001

Shaw, G. D., Conklin, M. H., Nimz, G. J., & Liu, F. (2014). Groundwater and surface water flow to the Merced River, Yosemite Valley, california:36cl and cl−evidence. *Water Resources Research*, *50*(3), 1943–1959. https://doi.org/10.1002/2013wr014222

Snyder, N. P., Rubin, D. M., Alpers, C. N., Childs, J. R., Curtis, J. A., Flint, L. E., & Wright, S. A. (2004). Estimating accumulation rates and physical properties of sediment behind a dam: Englebright Lake, Yuba River, Northern California. *Water Resources Research*, *40*(11). https://doi.org/10.1029/2004wr003279

"Surface Water Data for USA: USGS Annual Statistics. USGS Surface Water Data for USA: USGS annual statistics. (n.d.). Retrieved October 23, 2022, from https://nwis.waterdata.usgs.gov/nwis/annual?site_no=06019500&%3Bpor_06019500_80666=64915%2C00060%2C80666%2C1938%2C2022&%3Byear_type=W&%3Bformat=html_table&%3Bdate_format=YYYY-MM-DD&%3Brdb_compression=file&%3Bsubmitted_form=parameter_selection_list

Survey, U. S. G. (2015, February 5). *Chapter A6.3. specific conductance*. Techniques and Methods. Retrieved October 23, 2022, from https://pubs.er.usgs.gov/publication/tm9A6.3

Tockner, K., & Stanford, J. A. (2002). Riverine Flood Plains: Present State and future trends. *Environmental Conservation*, *29*(3), 308–330. https://doi.org/10.1017/s037689290200022x

Tóth, J. (1963). A theoretical analysis of groundwater flow in small drainage basins. *Journal of Geophysical Research*, *68*(16), 4795–4812. https://doi.org/10.1029/jz068i016p04795

Wegener, P., Covino, T., & Wohl, E. (2017). Beaver-mediated lateral hydrologic connectivity, fluvial carbon and nutrient flux, and aquatic ecosystem metabolism. *Water Resources Research*, *53*(6), 4606–4623. https://doi.org/10.1002/2016wr019790

Wetland Bank credits and fees. Wetland Bank Credits and Fees | MN Board of Water, Soil Resources. (n.d.). Retrieved October 24, 2022, from https://bwsr.state.mn.us/wetland-bank-credits-and-fees

Wilcove, D. S., Rothstein, D., Dubow, J., Phillips, A., & Losos, E. (1998). Quantifying threats to imperiled species in the United States. *BioScience*, *48*(8), 607–615. https://doi.org/10.2307/1313420

Williams, A. E., & Rodoni, D. P. (1997). Regional isotope effects and application to hydrologic investigations in southwestern California. *Water Resources Research*, *33*(7), 1721–1729. https://doi.org/10.1029/97wr01035

Yeh, H.-F., Lin, H.-I., Lee, C.-H., Hsu, K.-C., & Wu, C.-S. (2014). Identifying seasonal groundwater recharge using environmental stable isotopes. *Water*, *6(*10), 2849–2861. https://doi.org/10.3390/w6102849

Appendices: Raw Data

1. Temperature (℃)

Date	Location A	Location B	Location C	Location D	Location E	Ledford	Robb top	Robb
5/20/21	6.5	6.5			8.5	6.5		6.9
5/26/21	9.6	8.2	9.7	10.4	11	9.5		
5/27/21								8.9
6/18/21	20	19.5	20.2	21.4	22	18.4		18.5
6/24/21	19.7	19.1	19.2	19.3				
6/29/21						19.4		21.6
7/8/21	22.6	20.9	21	20.4	22.2			
7/14/21						17.4	20.1	20.7
7/20/21	19.6	18.4	18.5	20.3	20.5			
7/30/21						15.7	18.4	20.9
8/20/21	15.3	15.7	16.1	17	16.9			
8/28/21						10.8	12.7	15.6
9/11/21						14	15.4	17
9/19/21	15	12	11.5	11.7	11.7			
9/26/21						8.7	9.6	11.9
10/3/21	17	13.6	13.2	13.4	13.6			
10/10/21						5.6	5.9	6.1
10/17/21	12.4	10.1	9.3	10	10.2			
11/4/21	12.7	10.3	7.1	6.3	5.8	6.5	2.8	3.5

2. Specific Conductivity ($\mu S/cm$)

Date	Location A	Location B	Location C	Location D	Location E	Ledford	Robb top	Robb
5/20/21	374.2	368.2			389	767		551
5/26/21	390	384	404	415	419	726		
5/27/21								550
6/18/21	472	506	515	531	548	650		413
6/24/21	517	545	539	566				
6/29/21						654		394
7/8/21	508	555	555	571	577			
7/14/21						690	409	393
7/20/21	569	604	608	590	619			
7/30/21						726	425.4	393
8/12/21								
8/20/21	581	615	643	672	653			
8/28/21						835	481	439.5
9/11/21						774	450	418
9/19/21	645	704	716	705	740			
9/26/21						864	528	453
10/3/21	606	675	685	675	684			
10/10/21						989	600	593
10/17/21	667	711	748	726	744			
11/4/21	652	699	772	822	857	934	722	698

3. Flowrate (m^2/s)

Date	Location A	Location B	Location C	Location D	Location E	Ledford	Robb top	Robb
5/26/21						0.378		
5/27/21								0.248
6/2/21								0.282
6/3/21							0.307	
6/17/21						0.395	0.213	0.184
6/25/21	3.047	1.908	2.728	2.379	2.439			
6/29/21						0.391	0.152	0.129
7/8/21	2.442	1.694	2.357	2.240	2.398			
7/14/21						0.364	0.110	0.089
7/30/21						0.356	0.095	0.074
8/13/21			2.231	1.936	2.355	0.318		0.048
8/20/21	3.432	2.620	3.724	3.324	3.747			
8/28/21						0.358	0.074	0.052
8/31/21	2.030	1.526	2.121		2.163			
9/11/21						0.306	0.057	0.034
9/19/21	1.802	1.536	2.054	1.636	2.299			
9/26/21						0.304	0.056	0.042
10/3/21	1.827	1.578	2.350	2.722	3.198			
10/17/21	2.094	2.338	3.220	3.455	4.179			
11/4/21	2.076	2.151	2.625	3.072	3.975			

4. Stage (m)

Date	Location A	Location B	Location C	Location D	Ledford	Robb top	Robb
5/26/21					0.448		
5/27/21						0.494	
6/18/21							0.375
6/24/21						0.552	
6/29/21					0.515	0.466	0.314
7/14/21	0.786	0.774	0.713	0.744			
7/20/21					0.448	0.399	
7/30/21	0.744	0.759	0.686	0.722			
8/12/21					0.442	0.347	0.256
8/28/21					0.436	0.329	0.244
8/31/21	0.719						
9/11/21			0.680	0.710	0.439		0.216
9/19/21	0.665	0.847	0.777	0.820			
9/26/21					0.433	0.299	0.238
10/3/21	0.710	0.744	0.674				
10/10/21					0.424	0.271	0.219
10/17/21	0.698	0.747	0.674	0.677			
11/4/21					0.424	0.271	0.229

5. δ18O (0/00) VSMOW

Date	Location A	Location B	Location C	Location D	Location E	Ledford	Robb top	Robb
5/20/21	-17.3	-18				-18.3		-16.7
5/26/21	-18.5	-18.4		-18.3	-18.2	-18.4		
5/27/21								-18.3
6/2/21	-17.8	-18.6	-18.2	-18.1	-18.3	-18.6		-17.4
6/3/21	-18.9	-18.4	-18.6	-18.4				
6/17/21						-18.4		-18.4
6/25/21	-18.9	-17.7	-18.5	-18	-18.3			
6/29/21						-18.5	-18.4	-18.2
7/8/21	-18.6	-18.4	-18.2	-18.2	-18.3			
7/14/21						-18.7	-18.2	-18.2
7/30/21	-18.3	-18.5	-18.3	-18.3	-18.2			
8/12/21						-18.4	-18.3	-18.1
8/20/21						-19.1	-18.4	-18.4
8/28/21	-19.3	-19.3	-19.1	-18.8	-18.9			
8/31/21						-19.1	-19.1	-19
9/11/21	-19.4	-19.2	-19.1	-18.8	-18.9			
9/19/21 9/26/21	-19.3	-19.2	-19.1	-19	-19	-19	-18.5	-18.6

6. δD (0/00) VSMOW

Date	Location A	Location B	Location C	Location D	Location E	Ledford	Robb top	Robb
5/20/21	-137	-140				-138		-134
5/26/21	-139	-139		-139	-138	-139		
5/27/21								-139
6/18/21	-139	-142	-141	-140	-141	-140		-137
6/24/21	-142	-141	-141	-141				
6/29/21						-141		-139
7/8/21	-142	-141	-141	-141	-140			
7/14/21						-140	-140	-138
7/20/21	-140	-140	-140	-140	-140			
7/30/21						-139	-138	-137
8/20/21	-139	-140	-139	-140	-139			
8/28/21						-140	-139	-139
9/11/21						-140	-138	-138
9/19/21	-143	-143	-142	-141	-141			
9/26/21						-142	-141	-141
10/3/21	-146	-144	-144	-144	-143			
10/10/21						-142	-141	-141
10/17/21	-145	-145	-144	-144	-143			
11/4/21		-142	-141	-144	-144			-124